THE
PHYSICAL REVIEW
A Journal of Experimental and Theoretical Physics Established by E. L. Nichols in 1893
VOL. 52, NO. 1 JULY 1, 1937 SECOND SERIES

Sargent Curves for Artificially Radioactive Substances

ALLAN C. G. MITCHELL
Department of Physics, New York University, University Heights, New York, N. Y.
(Received March 25, 1937)

Sargent curves have been plotted for a number of elements whose end-points have been determined by extrapolation of the Konopinski-Uhlenbeck curves. The points lie on three smooth curves whose shapes agree with theoretical calculations based on the K-U theory. The relative values for the transition matrix moments are obtained and a discussion of the spins of the radioactive elements is given.

FOR some time data have been accumulating on the shape of the beta-ray curves for the artificially radioactive nuclei. There now exist fairly accurate data on some thirty substances and the form of the energy distribution curve as well as the value for the maximum energy of the emitted particles have been the subject of a large amount of experimental investigation. Tests have been made to see whether the original Fermi[1] theory of beta-ray emission or the modification proposed by Konopinski and Uhlenbeck[2] gives better agreement with the data. If one uses the method of treating the data due to Kurie, Richardson, and Paxton[3] it would appear that the K-U theory is in better agreement with experiment than the original Fermi theory. Furthermore, Kurie, Richardson, and Paxton showed that, while the energy distribution curve for certain elements may be fitted by a single K-U line, there are a considerable number of elements for which one must assume two K-U lines to account for the energy distribution. Further work by other investigators shows that this effect is quite common. One can account for this form of distribution curve by assuming that the active substance can disintegrate in two ways; (1) Directly to the ground state of the product nucleus with the emission of a beta-ray; or (2) to an excited state of the product with the emission of a lower energy beta-ray and the subsequent emission of one or more gamma-rays. The energy of the gamma-ray, if single, should be given by the energy difference between the end-points of the beta-ray curves. Up to the present, however, no single gamma-ray having an energy given by the difference in energy of the two beta-ray end-points has been found.

In compiling the data given in this paper the writer has used the criterion that the end-point must have been determined by the use of the K-U theory. This method has the advantage that it eliminates errors due to the sensitivity of the measuring instrument, since enough points may be accumulated at some distance from the end-point to determine this by extrapolation. Furthermore a distribution consisting of two components can be more readily recognized by

[1] E. Fermi, Zeits. f. Physik **88**, 161 (1934).
[2] E. J. Konopinski and G. E. Uhlenbeck, Phys. Rev. **48**, 7 (1935).
[3] F. N. D. Kurie, J. R. Richardson, and H. C. Paxton, Phys. Rev. **48**, 167 (1935).

TABLE I. *Observed limits, beta-ray spectrograph.*[7]

Element	Period	End-point Mev
P^{32}	14.5 d.	1.95
Mn^{56}	2.5 hr.	3.2
Br I	18 min.	2.00
Br II	4.2 hr.	2.05
Br III	36 hr.	0.85
Rh	44 sec.	2.5
Ag	22 sec.	2.7
I	25 min.	2.1
Ir	19 hr	2.2
Au	2.7 d.	1.15

this method than by any other. The disadvantage of the method lies in the possibility that the K-U theory may not be correct. Lyman[4] and Langer and Whitaker,[5] from a study of the beta-ray spectrum of Ra E with a high resolving power beta-ray spectrograph, and Paxton,[6] from an investigation of the spectrum of P^{32} in a cloud chamber, have come to the conclusion that, for various reasons, the extrapolated K-U end-point may be from 5 to 15 percent too high. This method of selection limits the data almost entirely to that taken using the cloud chamber. The results obtained by Alichanow, Alichanian, and Dzelepow[7] using a beta-ray spectrograph are shown in Table I, for sake of completeness, but are ruled out of the discussion since the end-points were determined by inspection.

The data on the various disintegrations are collected in Table II for electron emitters, and Table III for positron emitters. The radioactive element is shown in the first column, the reaction by which it was formed for the particular investigation under discussion in the second, and the half-life in the third. The fourth column lists the decay constants. For those elements which show only one mode of disintegration the decay constant is calculated from the well-known relation $\lambda = 0.693/\tau$. On the other hand for elements showing two modes of disintegration one must calculate the relative probability for each method of disintegration. Thus the decay constant for any mode of disintegration is proportional to the area under the distribution curve, i.e., a plot of $N(E)$ *vs.* E. The total probability of disintegration, which can be calculated from the half-life, is, of course, the sum of the partial probabilities for each mode of disintegration, so that $\lambda = \lambda_1 + \lambda_2$. For those elements showing two modes of disintegration sufficient data exist[8] to enable one to calculate λ_1 and λ_2 from a graphical integration under the distribution curves. The values obtained in this way are

[4] E. M. Lyman, Phys. Rev. **51**, 1 (1937).
[5] L. M. Langer and M. D. Whitaker, Phys. Rev. **51**, 713 (1937).
[6] H. C. Paxton, Phys. Rev. **51**, 170 (1937).
[7] Alichanow, Alichanian, and Dzelepow, Physik. Zeits. Sowjetunion **10**, 78 (1936).
[8] See references (a) and (c) in Table II.

TABLE II. *Electron emitters.*

Active Element	Reaction	Half-life	λ(sec.$^{-1}$)	End-point Mev	Reference
Na^{24}	(Na^{23}, D^2; Na^{24}, H^1)	15.5 hr.	1.24×10^{-5}	1.95	3, (a)
Si^{31}	(Si^{30}, D^2; Si^{31}, H^1)	145 min.	7.97×10^{-5}	2.05	3, (a)
P^{32}	(P^{31}, D^2; P^{32}, H^1)	14.5 d.	5.54×10^{-7}	2.15 (1.69)	(a)
Cl	(Cl^{37}, D^2; Cl^{38}, H^1)	40 min.	$1.45;\ 1.45\times10^{-4}$	1.5; 6.1	(a)
A^{41}	(A^{40}, D^2; A^{41}, H^1)	108 min.	$(0.503;\ 0.503\times10^{-4})$	1.5; 5	(a)
K^{42}	(K^{41}, D^2; K^{42}, H^1)	12.2 hr.*	$6.18;\ 9.58\times10^{-6}$	1.4; 4.4	(a)
B^{12}	(B^{11}, D^2; B^{12}, H^1)	0.02 sec.	3.46×10	13.0 (11.5 obs.)	(b)
Li^8	(Li^7, D^2; Li^8, H^1)	0.5 sec.	1.39	11.2 (10.0 obs.)	(b)
F^{20}	(F^{19}, D^2; F^{20}, H^1)	12 sec.	5.77×10^{-2}	5.9	(b)
N^{16}	(N^{15}, D^2; N^{16}, H^1)	9 sec.	7.70×10^{-2}	6.5	(b)
Mn^{56}	neutron capture	2.5 hr.	$5.48;\ 2.33\times10^{-5}$	1.2; 2.9	(c)
As^{76}	" "	26 hr.	$3.69;\ 3.71\times10^{-6}$	1.09; 3.4	(c)
In	" "	54 min.	2.14×10^{-4}	1.45	(c)
In	" "	13 sec.	5.32×10^{-2}	3.2	(d)
Ag	" "	22 sec.	3.15×10^{-2}	2.8	(d)
Rh	" "	44 sec.	1.58×10^{-2}	2.8	(d)
Dy	" "	2.5 hr.	7.7×10^{-5}	1.4	(d)
Cu^{64}	(Cu^{63}, D^2; Cu^{64}, H^1)	12.8 hr.	1.5×10^{-5}	0.83	(e)

(a) F. N. D. Kurie, J. R. Richardson, and H. D. Paxton, Phys. Rev. **49**, 368 (1936).
(b) W. A. Fowler, L. A. Delsasso, and C. C. Lauritsen, Phys. Rev. **49**, 561 (1936).
(c) M. V. Brown and A. C. G. Mitchell, Phys. Rev. **50**, 593 (1936).
(d) E. R. Gaertner, J. J. Turin, and H. R. Crane, Phys. Rev. **49**, 793 (1936).
(e) S. N. VanVoorhis, Phys. Rev. **50**, 895 (1936).
* H. Walke, Phys. Rev. **51**, 439 (1937).

probably reliable to within 10 or 15 percent. They are shown in column 4, and the corresponding end-points in column 5. The figures in parentheses in column 5 are the actual observed end-points for those cases in which the data seem sufficiently accurate for these figures to have meaning. The most accurately determined end-point of this group is that of P^{32} and the observed end-point given is that of Lyman[4] and Paxton.[6]

The data from Tables II and III are plotted on a Sargent[9] diagram in which $10+\log \lambda$ is plotted as ordinate against $\log E$ (E expressed in electron volts) as abscissa. Positron emitters are denoted by filled and electron emitters by open circles. It will be seen at once that the points fall reasonably well on three curves. Furthermore the positron emitters lie slightly higher than the electron emitters of the first group. The curves passing through the data are obtained in the following way. From the theory of beta-disintegration[10] it follows that

$$\lambda=(|G|^2/\tau_0)f(\epsilon_0) \tag{1}$$

and hence

$$\log_{10}\lambda=-\log_{10} C+\log_{10} f(\epsilon_0),$$

where

$$C=\tau_0/|G|^2. \tag{2}$$

Using the value of $f(\epsilon_0)$ for light nuclei obtained from

$$f(\epsilon_0)=(\epsilon_0^2-1)^{\frac{1}{2}}\cdot\left(\frac{1}{105}\epsilon_0^6-\frac{2}{21}\epsilon_0^4-\frac{247}{420}\epsilon_0^2-\frac{8}{105}\right)$$
$$+\tfrac{1}{2}\epsilon_0(\epsilon_0^2+\tfrac{1}{2})\log(\epsilon_0+(\epsilon_0^2-1)^{\frac{1}{2}}), \tag{3}$$

a table of values of $\log_{10} f(\epsilon_0)$ corresponding to values of $\log_{10} E$ (E is the experimental end-point in electron volts) can be constructed. From these data a curve of $10+\log\lambda$ *vs.* $\log E$ can be obtained which, by a suitable choice of the constant C, can be made to pass through the electron emitters of group I. Other values of the constant will give curves II and III, corresponding to forbidden transitions. The value of the constant C for curve I is 4×10^5 which, on the assumption that the matrix moment $|G|^2\approx1$ gives $\tau_0=4\times10^5$ sec. This value is somewhat larger than that given by Bethe and Bacher since their value was determined from the positron emitters. The ratio of the matrix moments for the three curves is

$$|G_{\rm I}|^2:|G_{\rm II}|^2:|G_{\rm III}|^2$$
$$=1:3.1\times10^{-2}:1.6\times10^{-4}.$$

Certain aspects of the graph deserve consideration. For a long time P^{32} appeared to be the only member of group III, thus giving the impression that the Sargent curves were not applicable to the light elements. With the addition of the high energy points for As^{76}, A^{41} and Cl group III is now quite well defined. A few discrepencies are apparent at once. The high energy end-point of Mn^{56} lies between curves II and III. The low energy end-point of A^{41} lies neither on curve I nor curve II, but the accuracy of this point is probably not high since the end-point was determined by resolving the distribution curve into two components. Finally the discrepancy between the observed end-point and that determined by the K-U method is shown for the elements B^{12}, Li^8, and P^{32}. Except in the case of P^{32} the discrepancies are not large. Since P^{32} is quite definitely a member of group III, it would appear that the method of using the extrapolated

[9] B. W. Sargent, Proc. Roy. Soc. **139**, 659 (1933).
[10] See H. A. Bethe and R. F. Bacher, Rev. Mod. Phys. **8**, 193–196 (1936).

TABLE III. *Positron emitters.*

Active Element	Reaction	Half-life	λ(sec.$^{-1}$)	End-point Mev	Reference
N^{13}	(C^{12}, D^2; N^{13}, n^1)	10.3 min.	1.12×10^{-3}	1.45	(a), (b)
F^{17}	(O^{16}, D^2; F^{17}, n^1)	1.16 min.	9.94×10^{-3}	2.4	(b)
O^{15}	(N^{14}, D^2; O^{15}, n^1)	126 sec.	5.53×10^{-3}	2.0	(b)
C^{11}	(B^{10}, D^2; C^{11}, n^1)	21.0 min.	5.5×10^{-4}	1.3	(b)
Cu^{64}	(Cu^{63}, D^2; Cu^{64}, H^1)	12.8 hr.	1.5×10^{-5}	0.79	(e)
Cl^{34}	(S^{33}, D^2; Cl^{34}, n^1)	33 min.	3.5×10^{-4}	3.0	(f)

(a) F. N. D. Kurie, J. R. Richardson, and H. D. Paxton, Phys. Rev. **49**, 368 (1936).
(b) W. A. Fowler, L. A. Delsasso, and C. C. Lauritsen, Phys. Rev. **49**, 561 (1936).
(c) M. V. Brown and A. C. G. Mitchell, Phys. Rev. **50**, 593 (1936).
(d) E. R. Gaertner, J. J. Turin, and H. R. Crane, Phys. Rev. **49**, 793 (1936).
(e) S. N. VanVoorhis, Phys. Rev. **50**, 895 (1936).
(f) R. Sagane, Phys. Rev. **50**, 1141 (1936).

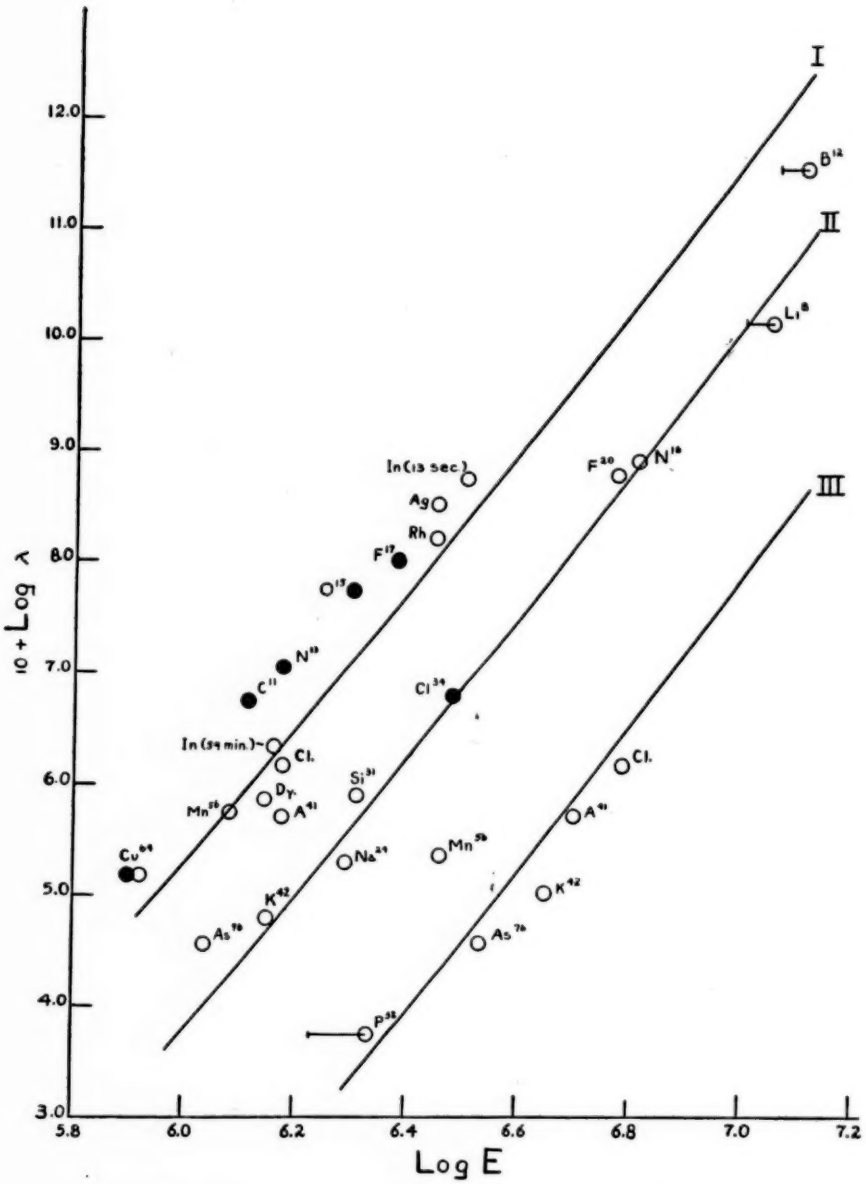

FIG. 1. Sargent curves for artificially radioactive elements.

K-U end-points is the best one for obtaining Sargent curves. Furthermore the theoretical curves of Fig. 1 were obtained from values of $f(\epsilon_0)$ derived from the K-U theory and the excellent agreement between the experimental points and the theoretical curves lends added confirmation to our belief that the K-U theory is essentially correct.

The three curves of Fig. 1 may be explained by considering the change of angular momentum of the system during emission of the beta-ray. If the change in angular momentum of the nucleus is given by $\Delta i = L$ curves I, II and III correspond to values of $L = 0$, 1, 2, respectively. Gamow and Teller[11] have proposed an alternative rule:

1. First Sargent curve: $\Delta i = 0$; proper functions even-even, or odd-odd.

2. Second Sargent curve: $\Delta i = 0$ or ± 1; proper functions even-odd.

[11] G. Gamow and L. Teller, Phys. Rev. **49**, 895 (1936).

There seems to be some ambiguity in assigning the correct proper functions to the nuclei in question. In what follows it will be supposed that the three curves are given by $\Delta i = L$, where i is the change in spin of the nucleus.

Now, one can suppose that all active substances listed in Table II can be formed from a stable isotope through the capture of a neutron, in which case the active element will differ in spin from its stable isotope by $\pm 1/2$.[12]

Table IV lists the atomic number, atomic weight and probable spin of the struck nucleus, excited nucleus and product nucleus, respectively, together with the value of Δi obtained from the Sargent curves. In most cases the value of the spin for the initial stable nucleus is known. The values of the spin for B^{11} and N^{15} were taken from the paper of Rose and Bethe,[13] and are shown in parenthesis, as are also assumed values for A^{40} and Si^{30}. Most of the product nuclei have even atomic numbers and atomic weights of the type $4n$ and consequently should have zero spin. Probable values for the spin of the excited nucleus can be worked out from the spin of the product and the value of Δi. In most cases this value will agree with one of the values obtained from the spin of the stable nucleus $\pm$ the spin of the neutron. When these values agree they are *italicized* in column 5 and considered to be spin of the excited nucleus.

It will be seen from Table IV that, in a large number of cases, reasonable values for the spin of the active nucleus can be obtained by assuming that the emission of gamma-rays on capture has no effect on the nucleus. Furthermore, this assumption gives a value for the spin of N^{15} in accord with the calculations of Rose and Bethe, and predicts a value of 1 for the spin of Si^{30}.

TABLE IV. *Possible spins.*

Stable Nucleus			Excited Nucleus			Product Nucleus		
Z	A	Spin	A	Spin	Δi	Z	A	Spin
$_{3}$Li	7	3/2	8	(1) (2)	1	$_{4}$Be	8	?
$_{5}$B	11	(3/2)	12	(1) (2)	0 (1)	$_{6}$C	12	0
$_{7}$N	15	(1/2)	16	(0) *1*	1	$_{8}$O	16	0
$_{9}$F	19	1/2	20	(0) *1*	1	$_{10}$Ne	20	(0)
$_{11}$Na	23	3/2	24	*1* (2)	1	$_{12}$Mg	24	(0)
$_{14}$Si	30	(0) 1	31	(1/2) *3/2*	1	$_{15}$P	31	1/2
$_{15}$P	31	1/2	32	(0) (1)	2	$_{16}$S	32	0
$_{17}$Cl	35 37	5/2	36 38	*2* (3)	0, 2	$_{18}$A	36 38	(0)
$_{18}$A	40	(0)	41	(1/2)	0, 2	$_{19}$K	41	3/2
$_{19}$K	41	3/2	42	(1) *2*	1, 2	$_{20}$Ca	42	(0)
$_{25}$Mn	55	5/2	56	*2* (3)	0, 2	$_{26}$Fe	56	(0)
$_{29}$Cu	63	3/2	64	(1) (2)	0	$_{30}$Zn	64	(0)
$_{33}$As	75	3/2	76	(1) *2*	1, 2	$_{34}$Se	76	(0)
$_{45}$Rh	103		104	—	0	$_{46}$Pd	104	
$_{47}$Ag	107 109	1/2 1/2	108 110	*0* (1)	0	$_{48}$Cd	108 110	0 0
$_{49}$In	113 115	9/2	114 116	4 5	0	$_{50}$Sn	114 116	(0) (0)
$_{49}$In	113 115	9/2	114 116	4 5	0	$_{50}$Sn	114 116	(0)
$_{66}$Dy	?	—	—	—		—	—	—

On the other hand Li, B, P, Cu and In cannot be made to fit into this simple scheme. For example In^{115} has a spin of 9/2 and the product nucleus Sn^{116} a spin of zero. The two periods of indium which have been most thoroughly investigated correspond to transitions lying on curve I for which $\Delta i = 0$, so that the process of gamma-radiation on capture must have accounted for a considerable change in spin. A similar supposition must be made to account for the behavior of the other four elements.

[12] Strictly speaking this statement is not correct since one should consider the change of angular momentum of the system due to the capture of the neutrons and also the fact that a gamma-ray is emitted when the neutron passes from a virtual level of the continuum to the quasi-stable excited state of the nucleus from which the disintegration occurs. Breit and Wigner (Phys. Rev. **49**, 519 (1936)) have shown that the most probable method of neutron capture is from the S wave, which means that the orbital angular momentum of the system does not change during the process. The change of spin on the emission of the gamma-ray, when the neutron passes from the virtual to the quasi-stable level, is something about which we have very little konwledge at present. It will be sufficient for the present discussion to make the assumption considered above and to see, if by this means, something can be said about the gamma-ray process.

[13] M. E. Rose and H. A. Bethe, Phys. Rev. **51**, 205 (1937).

Intensity Variation of L Series X-Ray Lines with Tube Voltage

GEORGE H. BANCROFT
Randal Morgan Laboratory of Physics, University of Pennsylvania, Philadelphia, Pennsylvania
(Received March 22, 1937)

The variation of intensity of the L series x-radiation, from a copper target, with the voltage applied to the x-ray tube has been studied. The voltage range over which this investigation was made included the K excitation value for copper. A definite increase was found in the slope of the intensity-applied voltage curve, which appeared immediately after the K state was excited. The intensity was plotted against the square of the voltage difference between the K excitation and the applied voltages, and the resulting curve was found to be substantially a straight line. This result is in accord with the theoretical predictions of Smekal and is an improvement over the experimental work of Stumpen.

SMEKAL[1] has pointed out, on a theoretical basis, that the intensity of x-radiation of any series should show increases as each harder series is excited successively by increasing the voltage on the tube. Experimental investigations of this prediction have been carried on by G. Kettmann,[2] A. Jönsson,[3] and H. Stumpen,[4] of whom the latter has done the most extensive work. Kettmann,[2] working on lanthanum L_α and L_β radiation, employed the photographic method, comparing the intensities obtained at different voltages by the use of a photometer. He was unable to find positive evidence of the increase in intensity predicted by Smekal.[1] A. Jönsson[3] used a Geiger point counter to measure the intensity variation of the L_α and L_β lines of molybdenum. The maximum value of the exciting voltage was 21 kilovolts. Since the K critical voltage for molybdenum is 19.9 kilovolts, Jönsson[3] obtained only two points on the line intensity tube voltage curve above the critical voltage value and the slope of the line passing through the two points did not depart obviously from that for points lying below. H. Stumpen,[4] using the ionization method for measuring intensities, studied the intensity variation with voltage of the tungsten L_β and L_γ lines. His curves showed a gradually increasing slope beginning at about 70 kilovolts whereas the K excitation voltage for tungsten is 69.9 kilovolts. Further, he reported that the intensity above this point increased linearly with the square of the applied voltage. These facts are summarized in Table I. Compton and Allison[5] say, in their discussion of this work, that, "Although such an effect was predicted by Smekal,[1] Kettmann[2] failed to find positive evidence for it and experimentally its existence does not seem to be satisfactorily demonstrated."

The work of E. Lorenz,[6] on the voltage intensity relation for the aluminum K series showed that no such increases in intensity were to be expected where there was no possibility of exceeding the critical potential of a harder characteristic radiation. Theories of collision ionization, such as those of Davis,[7] Rosseland,[8] Thomas,[9] Webster[10] and others[11] have been limited to the investigation of the direct excitation of a single level by electron impact; hence they could not be expected to offer any explanation of an increase in intensity connected with the critical potentials of harder characteristic radiation.

The investigation described in this paper was undertaken to obtain additional experimental evidence concerning the behavior of the intensity of a group of x-ray lines of the L series when the critical K voltage of the same element was exceeded. The method used to estimate these

[1] A. Smekal, Verh. d. D. Phys. Ges. **21**, 149 (1919).
[2] G. Kettmann, Zeits. f. Physik **18**, 359 (1923).
[3] A. Jönsson, Zeits. f. Physik **43**, 845 (1927).
[4] H. Stumpen, Zeits. f. Physik **36**, 1 (1926).
[5] Compton and Allison, *X-Rays in Theory and Experiment* (D. Van Nostrand Co. 1935), p. 81.
[6] E. Lorenz, Zeits. f. Physik **51**, 71 (1928).
[7] Bergen Davis, Phys. Rev. **11**, 433 (1918).
[8] Rosseland, Phil. Mag. **45**, 65 (1923).
[9] Thomas, Proc. Cam. Phil. Soc. **23**, 829 (1927).
[10] Webster, Hansen, and Duveneck, Phys. Rev. **43**, 839 (1933).
[11] Reference 5, page 73.

TABLE I. *Variation of intensity with tube voltage.*

RADIATION STUDIED	MAXIMUM VOLTAGE	METHOD OF INTENSITY MEASUREMENT	VOLTAGE SUPPLY	AUTHOR
Lanthanum L_β L_α	1.03 V_k=39.9 kv 1.08 V_k=41.9 kv	Photographic	Induction machine	Kettmann[2]
Tungsten L_β L_γ	1.323 V_k=90.0 kv 1.323 V_k=90.0 kv	Ionization Ionization	500-cycle a.c. Unrectified	Stumpen[4] Stumpen[4]
Molybdenum L_α L_β	1.055 V_k=21.0 kv 1.055 V_k=21.0 kv	Geiger Point Counter	500-cycle a.c. Rectified and filtered	Jönsson[3]

intensities, was to measure the photoelectric current obtained from an insulated metal plate, which was placed in the path of x-rays. The number of photoelectrons ejected from the surface per second was proportional to the number of x-ray quanta striking it in that time interval.

THE EXPERIMENTAL ARRANGEMENT

The high voltage for the x-ray tube was obtained by transforming the regular 60-cycle a.c. supply. The high voltage thus obtained was rectified by the use of a full wave, four kenotron, bridge circuit the output of which was further smoothed by two 0.1 microfarad condensers. A resistance of 50,000 ohms was used in series with the x-ray tube to reduce the effect of any unavoidable arc due to the liberation of gas. The voltage was measured in terms of the current flowing through ten, one megohm, Shallcross, precision, wire wound resistors connected in series.

The x-ray tube was mounted directly on the spectrograph as shown in Fig. 1, and was sealed in position with sealing wax. No window was used between the x-ray tube and the spectrograph, both of which were separately connected to the pumping system, which was of a standard type. Electrode holders, provided with sylphon adjustments *H–H*, were fitted to the ground ends of the Pyrex separator tube as shown in the figure. These adjustments provided a limited motion for each of the electrodes back and forth along the axis of the tube and thus made it possible to bring the focal spot and the collimating system of the spectrograph into accurate alignment. The motion of the cathode made possible a limited external control of the size and uniformity of the focal spot. The actual cathode was of the indirectly heated, oxide-coated type. Around this cathode a focusing shield was placed. By adjusting the distance between the surface of the cathode and this shield almost any degree of focusing could be obtained. The anticathode was water cooled and was provided with an internal baffle which constrained the water to flow smoothly and continuously across the rear surface of the target face.

A small, plane, ruled glass grating, having 2406 lines per inch was used. The ruled surface was approximately 2.5×8 mm, and the grating was mounted so that the axis of rotation passed along the ruled surface. A knife edge, which was brought up quite close and parallel to the ruled surface, formed the second slit of the collimating system of the spectrograph. This slit was 0.220 mm in width, whereas the first slit was 0.275 mm wide. The last slit S_3, which selected the radiation desired, was situated at a point about 15 cm from the grating and was 0.990 mm wide. Immediately behind this last slit, a small nickel vane *B* was introduced through the wall of the spectrograph by the use of a ground glass joint, in such a way, that it could be set parallel or perpendicular to the x-ray beam, thus either allowing the beam to pass or cutting it off completely from the rest of the spectrograph chamber. This vane was electrically connected to the grounded case of the spectrograph. The purpose of the vane was to allow the comparison of the position of the galvanometer spot, with and without the x-ray beam affecting the measuring circuit. An ion trap *C* was arranged as shown

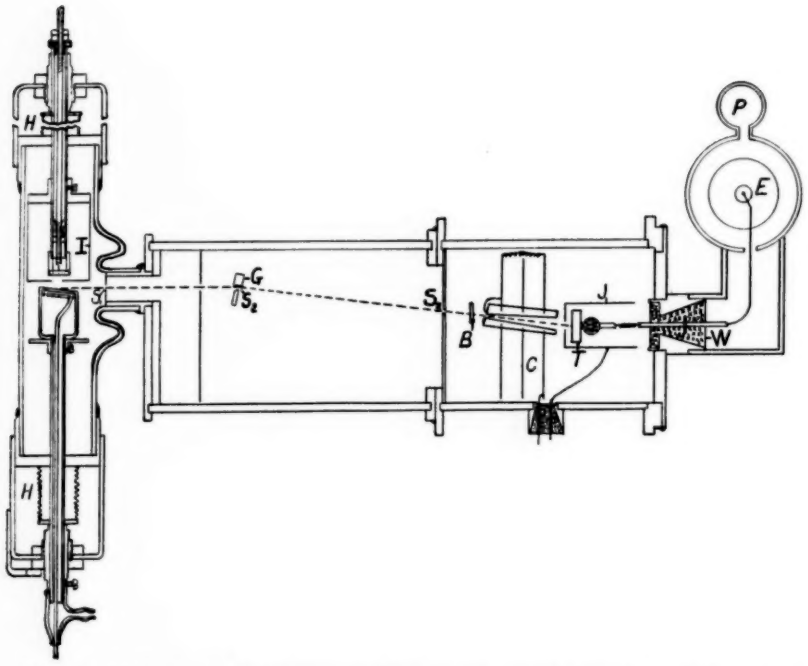

FIG. 1. A diagram of the x-ray tube, vacuum spectrograph, and detecting device used.

in Fig. 1, between the vane B and the rest of the chamber. The almost parallel plates through which the x-ray beam passes were purposely made to diverge in the direction away from the source in order both to prevent deflection of the beam by reflection and to minimize the generation of photoelectrons. A potential difference of about 90 volts was maintained between these plates, as is indicated in the figure. Having passed through the ion trap, the x-rays struck an insulated metal plate T, having an aluminum surface, and photoelectrons were produced. These photoelectrons were then swept out of the area by the field from a positive electrode J, and the insulated plate charged up positively as more and more electrons were lost. The charge from the insulated plate was conducted out of the spectrograph through the sealing wax plug W in the back plate. From this point the charge was carried to the control grid E, of the Western Electric electrometer tube D96475, by means of a semi-rigid conductor passing through brass shields with air as the insulator.

The electrometer tube was used in a Barth[12] circuit as modified by Pennick.[13] The galvanometer read the difference in voltage between the plate and the screen grid of the tube, produced in response to changes in the potential of the control grid. The circuit was tested for linearity of voltage response by the application of a number of known voltages, obtained from a Leeds and Northrup student potentiometer, calibrated in the usual manner, and it was found to be accurately linear for voltage changes as great as 0.04 volt. A rough potentiometer system P was permanently connected in the circuit between the ground and the high grid resistance, which made it possible to check the sensitivity of the circuit from time to time.

EXPERIMENTAL PROCEDURE

In the adjustment of the spectrograph, the position of the anticathode was first set visually, with the help of a carbon arc light focused upon the target at the place where the focal spot would later be formed. Then a series of photographic exposures were made with the x-rays, in which the position of the anticathode and the angle of the grating were separately adjusted until the most desirable diffraction pattern was obtained. The copper L group was identified

[12] Barth, Zeits. f. Physik **87**, 399 (1934).
[13] Pennick, Rev. Sci. Inst. **6**, 115 (1935).

and the slit S_3 was adjusted to isolate it. The ion trap and the photoelectric plate with its accompanying anode were then placed in position. Photographic plates were exposed to make certain that the beam was passing by each new obstruction without change and was actually striking the photoelectric plate. The action of the vane was also checked by a photographic method.

The electrometer tube circuit was set up and adjusted according to the instructions of Pennick.[13] The plate voltage, picked from the filament circuit, was set so that the flat portion of the galvanometer deflection-filament current curve fell accurately, at the rated filament current (270 ma). The circuit was supplied with 24 volts from four 6 volt, 120 ampere-hour, lead storage batteries. The sensitivity of the circuit was approximately 15,000 mm per volt, which, with a grid resistor of 9.6×10^{11} ohms, gave a current sensitivity of the order of magnitude of 6.9×10^{-17} amperes per mm. The circuit was found to have a period of three minutes for full deflection, but on investigation of the time rate of deflection, it was found that, for the magnitude of the deflection usually obtained, 85 percent of the total movement took place in the first minute. Also, if the time interval were carefully controlled, the deflections at the end of a minute were reproducible, and it was therefore considered legitimate to read the deflections after the x-rays, in each case, had been falling on the plate for one minute. The time necessary to take a full curve was thus reduced to three hours. This shorter time was advantageous since the possibility of keeping the conditions in the x-ray tube reasonably constant while a curve was being observed was thus increased. The current through the x-ray tube was kept constant throughout an observation to within 0.2 ma or 2 percent, by manipulation of a resistance in the cathode heater circuit. It was found that more stable operation was obtained when the voltage on the x-ray tube was immediately brought up to its maximum value and then reduced in the steps desired to obtain the intensity voltage curve.

After a few hours of operation the anticathode surface became roughened. The anticathode was then removed and its surface was either polished down, or replaced if it were too thin. At the same time the cathode was removed and given a fresh coating. Each time the electrode positions were disturbed a readjustment was necessary to assure a proper focus and a proper alignment of the focal source with the entire slit system. In order to make this adjustment, the x-ray tube was operated and the deflection of the galvanometer at a particular voltage was recorded. The anticathode was then moved along the axis of the tube in 0.1 mm steps and the galvanometer deflections were observed at the same voltage for each position until a maximum had been passed through. At this adjustment a small piece of photographic plate was fastened to the vane B and a photographic check was obtained. Care was always taken to have a fresh coating on the cathode and a fresh area of anticathode surface for the focal spot, for each curve taken. The cathode structure was just eccentric enough to move the focal spot to a new position if it were rotated through 180°. The separation of the focal spots thus obtained was as much as two or three mm. In this way it was possible to use the same polished surface of the anticathode to obtain two curves.

Results

The spectrograph, as used, had a rather low dispersion and the whole group of copper L lines was selected by the final slit, instead of only one line of the group. However, if the intensity of the L lines is to be increased due to the emission of K radiation, according to the Kossel hypothesis, then those lines arising from vacancies in either the L_{II} or the L_{III} level should experience an increase in intensity and the total increase should be greater than if only a single line were observed. It was, consequently, thought best to use the entire L group for the intensity measurements.

A number of curves, of which those in Fig. 2 are typical, were obtained, showing the behavior of the intensity with increasing voltage, in the neighborhood of the K critical potential. Each point on the curves represents the average of six separate evaluations of the intensity at that voltage. In Fig. 2 the individual values are shown by the small dots and the average values by the

dots with circles around them. All of the curves exhibit a definite increase in slope above the K excitation point. If the intensities above the K critical potential are plotted against $(V-V_k)^2$, the resulting curves are substantially straight lines, as may be seen in Fig. 3. If these intensities

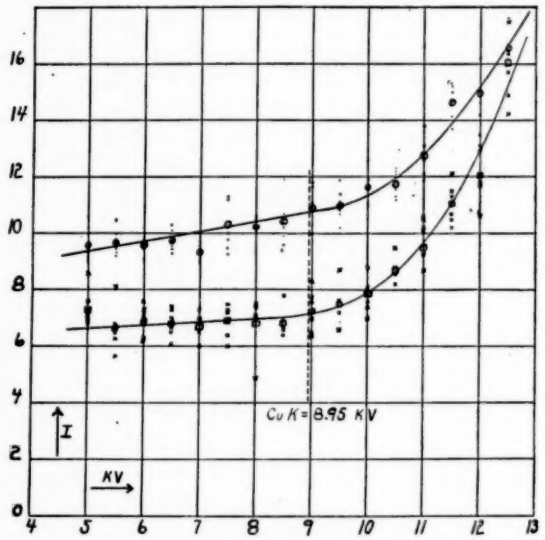

FIG. 2. The intensity of the group of Cu L lines plotted directly against the voltage applied to the x-ray tube. The ordinates represent the galvanometer deflection in cm.

are plotted against the square of the voltage applied to the tube, the resulting curves are definitely not straight lines. If it is assumed that the increase observed is due to atoms left ionized in the L state after the emission of K radiation, then one should expect that this increase would follow the same law as is obeyed by the K radiation itself. Since the law obtained from the curves in Fig. 3 agrees very well with this theoretical expectation, one may reasonably conclude that the portion of the intensity due to direct collision ionization remains roughly constant over the region investigated, which lies above the K excitation potential.

The effect of a change in the distribution of the intensity of the electronic bombardment of the focal spot was shown by a curve (see Fig. 4), taken in an effort to repeat a set of observations, after varying the voltage from the maximum to the minimum value, by changing it in the reverse direction from the minimum back to a maximum again. Between six and seven kilovolts on the return curve a sharp break occurred after which the course followed was approximately parallel to that taken in the original set of observations and was displaced from it in the direction of reduced intensity. This break was correlated with a quite noticeable change in the character of the focal spot. During the first set of observations the focal spot possessed three quite definite areas and, at the break in the curve, one of these areas was seen to disappear. During the remainder of the repeat curve the character of the focal spot remained constant. In accordance with the results of this test all curves showing irregularities were discarded.

The curves obtained (Fig. 2) show increases of intensity over that at the critical voltage varying from 54 percent to 128 percent over the voltage range employed. This increase appears to begin close to the critical voltage for K excitation. The curves also seem to have flattened out somewhat, before ten times the L critical potential of 950 volts is reached as judged from the portion of the curve below the K critical value. This seems to be in qualitative agreement with the results of Lorenz on the Al K_α line.

The results reported in this paper agree with those of Kettmann,[2] Stumpen,[4] and Jönsson,[3] insofar as they indicate an increase in the intensity of the L group when the K excitation voltage is exceeded. However, they are in definite disagreement with those of Stumpen[4]

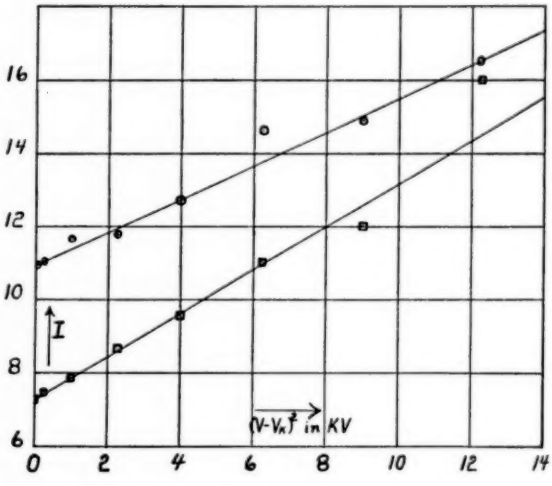

FIG. 3. The intensity of the group of Cu L lines plotted against $(V-V_k)^2$. The ordinates represent the galvanometer deflection in cm.

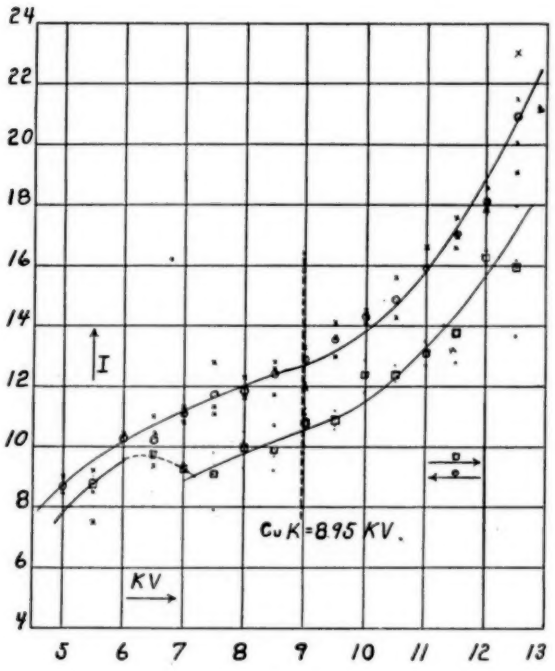

FIG. 4. The intensity of the group of Cu L is plotted against the voltage applied to the x-ray tube and shows the effect of a change of the distribution of the intensity of electron bombardment in the focal spot of the tube. The change coincides with the break in the curve.

in that the intensity is not proportional to the square of the applied voltage but to the square of the difference between the K critical potential and the applied voltage. The conditions employed in this investigation may be considered as exceptionally favorable for the determination of this relation, as the maximum in the intensity voltage curve, reported by E. Lorenz, occurs in approximately the region in which the increase in intensity begins. Hence the increase is added to a practical horizontal portion of the curve, instead of to a portion of the curve which is normally rising at a rapid rate, as was the case in the work of Stumpen.[4] These results would seem to agree very well with the predictions of the theory of Smekal,[1] concerning the return of the excited atom to its normal state.

At this point I wish to express my thanks and appréciation for the many suggestions and the continued interest of Dr. C. B. Bazzoni, under whose direction this investigation was carried out, and to the Randal Morgan Laboratory of Physics of the University of Pennsylvania, whose laboratory facilities were placed at my disposal, thus making this work possible.

JULY 1, 1937 PHYSICAL REVIEW VOLUME 52

High Potential Apparatus for Nuclear Disintegration Experiments

H. R. CRANE
University of Michigan, Ann Arbor, Michigan

(Received April 26, 1937)

A 1,000,000-volt transformer and vacuum tube apparatus for nuclear disintegration work is described. The transformer consists of five 200,000-volt sections, in a cascade circuit. The tube is made of five heavy Pyrex glass sections 24 inches long and 16 inches in diameter, with hollow steel electrodes 6 inches in diameter. Each accelerating gap in the tube is connected across one of the sections of the transformer to insure uniform potential distribution. A focused ion beam of 250 microamperes is obtained at the target. Cloud chambers are operated in synchronism with this apparatus by means of a common contact system, in such a way that both the ion source and the transformers are energized for only about $\frac{1}{2}$ second, during which the chamber expansion takes place.

INTRODUCTION

SINCE the beginning of research in nuclear physics the principal technical problem has been the acceleration of positive ions, and to this end a number of different methods have been developed and used. One of the simplest and most direct, although perhaps not the most inexpensive, ways of accelerating positive ions is the application of a high alternating potential from a transformer to a vacuum tube. The high potential end of the tube will then be alternately positive and negative, and the ions will flow to the target only on the positive half-cycle. Nothing at all will happen during the negative

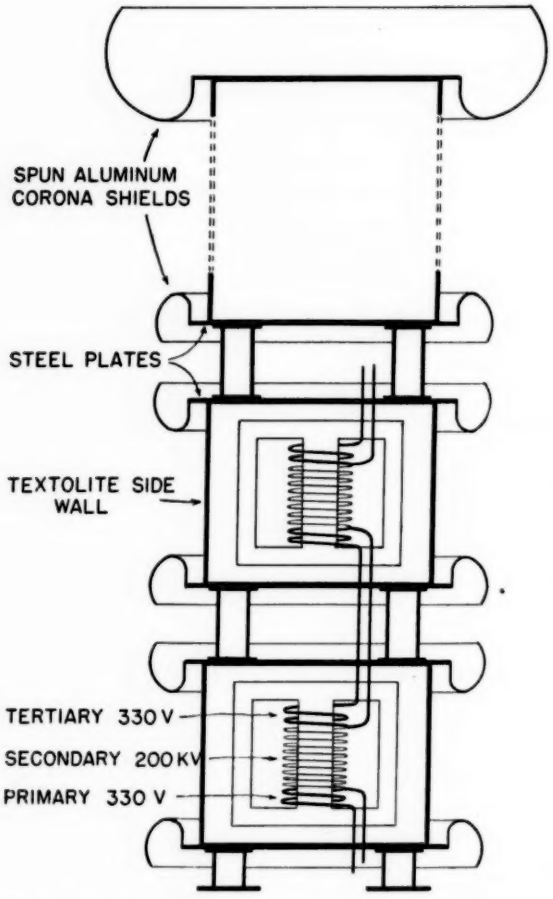

FIG. 1. Cross section of the transformer stack, with windings indicated schematically.

half-cycle, provided there are no free electrons available at the negative end of the tube. In spite of the sine variation of potential with time, an ion beam which is nearly homogeneous in energy can easily be obtained by means of a bias voltage in the source or a synchronous shutter in the ion beam itself, arranged so that ions flow only when the potential is near the peak value, say for approximately $\frac{1}{4}$ of the cycle. Even with this interrupted flow of ions, large average currents can be obtained, because of the practically unlimited power available in this type of apparatus.

The field of application of the alternating potential apparatus is not universal. There exists, however, a large and important class of problems in nuclear physics for which accurate control and measurement of the ion velocity are not essential. As examples we may mention studies of the energy spectra of gamma-rays, beta-rays, neutrons, protons and alpha-particles emitted by nuclei, and studies of the secondary effects produced by these high energy radiations and particles. In these cases the properties of the radiations studied are determined by the structure of the nuclei and are, within reasonable limits, not sensitive to the energy of the bombarding particles in the ion beam. The alternating potential apparatus is particularly suited to problems of this class. Problems such as the absolute measurement of the efficiency of disintegration, and of resonance levels for capture of particles by nuclei cannot be attacked with the apparatus to be described, but could be brought within its scope by the addition of a magnetic separator to monochromatize the ion beam. By somewhat specializing the scope of the present apparatus, valuable compensating advantages in the direction of simplicity, dependability and high ion current have been obtained, as will be evident from the following description.

DESCRIPTION

Transformer[1]

The foremost thought in outlining the requirements for a high voltage transformer was to have available a number of terminals of intermediate voltage, so that a definite distribution of potential along the tube could be maintained. The transformer set was therefore made to consist of five separate units, connected in a cascade circuit, as indicated schematically in Fig. 1. By means of air gaps in the cores of the units, the reactance of the system was approximately adjusted (at the factory) to the capacitance of the load, so as to obtain a favorable power factor in the primary feed circuit. Although the charging current flowing between the transformer and the tube is of the order of 100 milliamperes at 1,000,000 volts, the current in the primary circuit is only about 35 amperes at 330 volts. The actual power consumed by the system is mainly due to the iron and copper losses in the transformer itself; the corona and ion beam loads are both comparatively small. The total power consumed is about 6 kilowatts at full voltage.

[1] Designed and built by the Westinghouse Electric and Manufacturing Company.

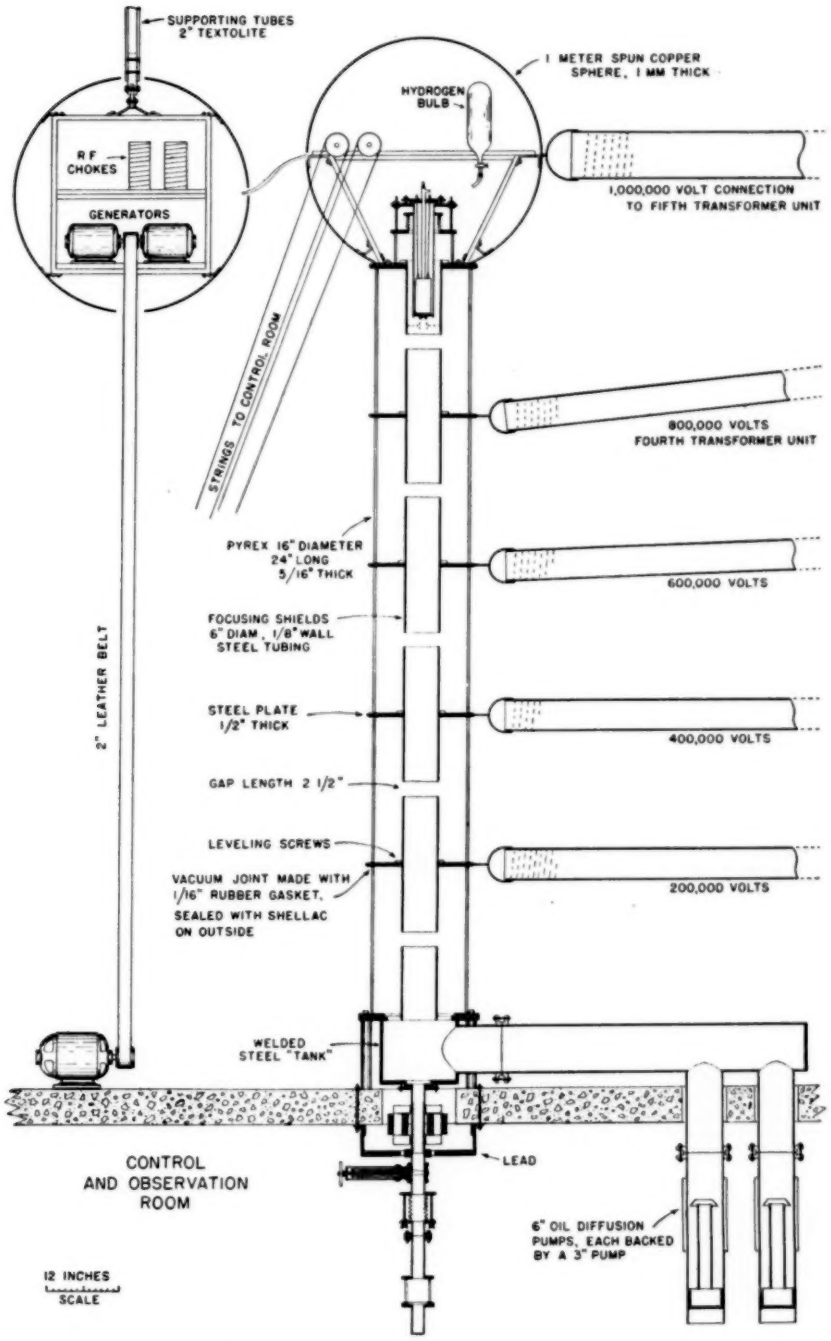

FIG. 2. Scale drawing of the entire tube.

A continuously variable voltage for exciting the primary of the transformer is obtained from a motor driven induction regulator, which supplies 10 kilowatts at any desired voltage between 110 and 330 volts. An overload relay breaks the primary circuit when the vacuum tube becomes "soft," and acts so quickly that no primary resistance is necessary for protection against excessive currents.

Vacuum tube

The vacuum tube is built of five Pyrex glass cylinders 16 inches (about 41 cm) in diameter and 24 inches (about 61 cm) long, with wall

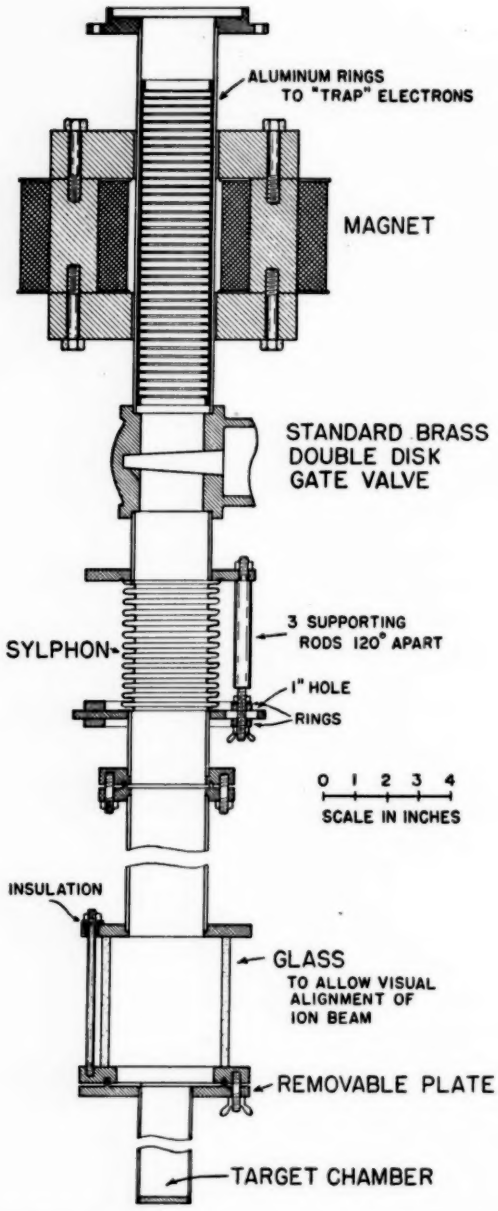

FIG. 3. Detail drawing of the ion pipe at the lower end of the tube.

thickness ranging from $\frac{1}{4}$ to $\frac{3}{8}$ inch (about 8 mm). The choice between glass and porcelain was mainly determined by availability and cost. The principal advantage which the commercially available porcelain has to offer over glass is that its outer surface is corrugated. This increases its strength against external flash-over and allows a shorter tube to be used for a given voltage. Where space is at a premium this can become an important advantage, but the height of the room in which the present tube was built was sufficient to permit the use of a straight walled tube. The fact that the ion path in a straight walled tube is necessarily as much as 50 percent longer has been found, in the author's experience, to be of secondary importance. The strength of the $\frac{1}{4}''$ glass wall against puncture due to flashes from the internal electrodes to the outside is entirely sufficient in a glass tube of the present dimensions, operated at 200,000 volts per section. For considerably higher potentials per section porcelain is undoubtedly preferable because of its thicker walls (usually $\frac{3}{4}$ to $1''$). Glass cylinders may, however, be made to withstand higher potentials by increasing their diameter in relation to the diameter of the accelerating electrodes, as well as increasing their length. The increase in diameter reduces the concentration of electrical stress in the neighborhood of the accelerating gap.

Electrode arrangement and focusing

The hollow electrodes through which the ions are accelerated are made of 6 inch (15 cm) diameter seamless steel tubing, $\frac{1}{8}$ inch (3 mm) in wall thickness. The gaps which support the 200,000 volts difference of potential are 2.5 inches (6.3 cm) long. The edges of the steel tubes are simply rounded, so that they have a radius of curvature of $\frac{1}{16}$ inch. No trouble has yet been experienced due to electron emission from these edges under the influence of the high field, so it appears that the attachment of rings of larger radius of curvature to the ends of these tubes is unnecessary up to the voltage used.

It will be noticed in Fig. 2 that the ion source is insulated from the first 6 inch electrode surrounding it, by means of an 8 inch glass cylinder inside the sphere. This was done so that an extra accelerating gap could be provided immediately below the source as shown by the dotted lines, with an adjustable potential of 5 to 10 kilovolts for focusing. This is not ordinarily used, because the system is approximately in focus without it. The focal spot obtained without the extra focusing gap is about 1 inch in diameter, and is reduced to less than $\frac{1}{2}$ inch by the use of the extra focusing gap. The small focal spot would be necessary if a magnetic analyzer were to be used.

Unsteadiness in the position or focus of the ion beam due to uneven and changing electrostatic charges on the inner glass walls of the tube seem to be small, with the length of accelerating gap used at present. The remedy for any effect of this kind would of course be to place a metal shield around the first accelerating gap so that charges on the glass could not attract the moving ions. No such shields would be necessary in the succeeding gaps, due to the higher velocity of the ions.

At the bottom of the tube (see Fig. 3) a magnet is provided for deflecting out of the beam any electrons which are accelerated on the negative half-cycle. A series of aluminum annular rings in the tube serve as traps for the electrons. Some system of baffles of a substance of low atomic number is absolutely essential to stopping the electrons: we have found that in a smooth walled brass tube a large fraction of the electrons arrive at the target in spite of a strong magnetic field. This is undoubtedly due to the efficient reflection of electrons of this energy by substances of medium or high atomic number. As an interesting experiment we have "piped" a stream of 1 Mev electrons around a corner by means of a piece of lead pipe, with surprisingly little loss.

Ion source

The ion source is one which has gradually developed out of a type already described.[2] The principal new features of the present one are that the anode is in the shape of a ring immediately surrounding the end of the canal, and that nearly all of the inside surface of the source is of glass, as shown in Fig. 4. This results in considerably larger ion currents than were obtained from the previous type, in which most of the inside surface was of metal, at anode potential. As a result of trying a number of arrangements it has appeared that the locations of the filament and anode with relation to the canal are not of great importance, probably because during operation a plasma condition exists, and the entire volume is filled with a cloud of ions. The location of the anode around the canal,

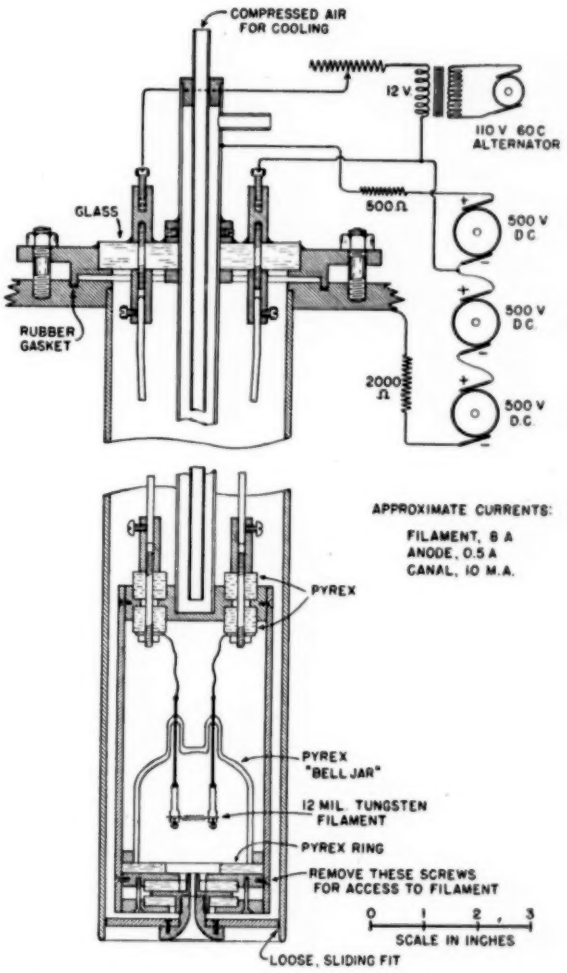

FIG. 4. Ion source assembly, with the electrical circuit shown schematically. The two 500 volt generators which supply power to the anode are sometimes replaced by a transformer, connected to the tertiary winding of the top transformer unit, as described in the text.

however, gave the greatest yield of ions, which indicates that the cloud of ions is somewhat more dense in this region than in other parts of the volume.

An important characteristic of the operation of this source is that for every gas pressure there is an optimum filament temperature, and that the ion current falls off on both sides of this value. The following explanation seems to fit the facts: The negatively charged canal causes an ion sheath to be formed around itself, which may take various forms, as indicated in Fig. 5, according to the density of ions in the discharge, which is in turn determined by the gas pressure, filament emission etc. As the filament emission is

[2] Crane, Lauritsen and Soltan, Phys. Rev. **45**, 507 (1934).

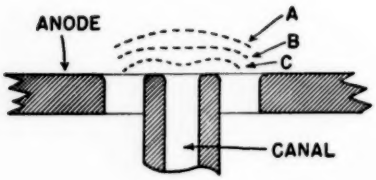

FIG. 5.

increased, the ion density in the space increases, and the sheath changes its form from *A* through the flat form *B*, to *C*. The ions which leave the lower surface of the sheath have initial directions perpendicular to the sheath. Therefore under conditions in which the sheath is flat across the end of the canal the ions will escape through the canal in an initially parallel beam. External focusing conditions in the accelerating tube may, however, require an initially diverging or converging beam. In this case the current received at the target will be a maximum when the filament emission is adjusted so as to fulfill those particular conditions. Thus it may be that, within narrow limits, adjusting the filament emission actually amounts to adjusting the focusing conditions. In actual operation the maximum in the ion current is easily attained and is broad enough so that frequent adjustment of the filament current is not required.

The ratio of atomic to molecular hydrogen ions has not been measured directly, but according to disintegration results it is considerably more favorable than in the previous source. This is probably due to the fact that the inside surfaces of the source are almost entirely of glass, which, if clean, reduce the rate of recombination of atomic hydrogen, and also give off smaller amounts of gases of other kinds, under heat and bombardment.

Taking advantage of the fact that the fifth unit of our transformer stack is equipped with a tertiary winding of 330 volts, we are able to supply the anode of the ion source with alternating current which is in phase with the high voltage on the accelerating tube. The 330 volts is stepped up to about 1500 volts by means of a small transformer. On the negative half-cycle (top of the tube negative) both the canal and the anode are negative with respect to the filament, so no current at all flows in the discharge space. It is therefore possible to double the power in the discharge during the positive half-cycle without greater heating effect than would be obtained normally with direct current on the anode. The total absence of discharge in the source on the negative half-cycle has the further advantage of reducing the small number of electrons which inevitably leave the region of the source and accelerate down the tube on the negative half-cycle.

The rate at which hydrogen is admitted to the source is such that the pressure in the accelerating tube rises from 10^{-5} to between 5×10^{-5} and 10^{-4} mm during operation.

The total ion current which is obtained at the target regularly and dependably is 250 microamperes. Under the best conditions about 50 percent more than this is obtained. This is measured in a Faraday cage about 3 cm in diameter and 15 cm deep, and probably includes very little current due to secondary electrons.

Protection against corona and sparking

The principal reason for enclosing the top of the tube in a sphere and enclosing the ion source generators in an elongated sphere was to prevent sparking to the walls and ceiling of the room, which are only about 9 ft. from these high voltage surfaces. Four spun copper hemispheres 50 cm in radius and 1 mm in wall thickness form the sphere on the tube and the "blimp" enclosing the generators. The five connectors between the tube and transformer consist of cardboard tubing 5″ in diameter (except the top connector, which is 8″ in diameter), space wound with fine wire and enameled. These accomplish a double purpose in that sparking between connectors is prevented because of their large radius of curvature, and electrical surges from the tube are not transmitted to the transformers because of their inductance. The distance between the transformer stack and the tube is 10 ft., which is sufficient to prevent a direct spark-over along the inductive connectors.

Corona discharge is practically eliminated by the large radii of curvature of the high potential surfaces. Therefore the external load on the transformer is almost a pure capacity (out of phase) load. In the present apparatus this causes the voltage to build up to a value somewhat in excess of that calculated from the

primary voltage and the turns ratio. We have counteracted this effect by placing a resistance (heater) across the tertiary winding of the top unit, which consumes about one kilowatt and constitutes an in phase load. Thus in this particular instance the corona power loss which is so completely eliminated by the rounded surfaces has to be replaced by an artificial in phase load. The charging current which flows between the transformer and the spheres is roughly 100 milliamperes, at 1,000,000 volts. Although this circulating current is very large compared to the useful current drawn by the ion beam, it does not represent power loss.

Operation of the tube in synchronism with the cloud chamber

In operating the tube and cloud chamber in conjunction, there is no necessity for running the tube or the ion source during the time between expansions of the chamber. A central motor driven electrical contact system is used to operate the cloud chamber, transformer and tube. The primary circuit of the transformer and the anode circuit of the ion source are closed for about $\frac{1}{2}$ second at the time the chamber expands. In studying delayed activities of short life, the contacts are simply shifted so that the bombardment precedes the expansion by any desired length of time.

Discussion

Finally, some brief remarks about the possibilities of working at higher voltage with alternating potential apparatus of the type described may be of interest. At 1,000,000 volts the charging current to the high potential parts of the transformer and vacuum tube is necessarily of the order of 100 milliamperes. This current is proportional to the product of the voltage, capacity and frequency. The size of the apparatus required (and hence its capacity) is larger for higher voltages. Therefore in building apparatus for greater maximum voltage, the charging current may be expected to rise more nearly as the square than as the first power of the voltage. Although high charging current does not necessarily mean high power consumption, it does require that the transformer have a large current carrying capacity, and therefore the cost of the transformer goes up very rapidly with the voltage above 1,000,000 volts. In spite of the fact that the construction of apparatus of this type for voltages considerably higher than 1,000,000 is straightforward from the engineering standpoint, it is clear that an economic limit is reached at a point not far above 1,000,000 volts.

As a result of our experience with the present apparatus we believe that some advantage would be gained by placing the vacuum tube and transformer stack close together, eliminating the inductive connectors, and by placing the ion source generators on top of the transformer stack. The resulting reduction in the capacity-to-ground of the system would be desirable at 1,000,000 volts, and would probably be essential at higher voltages. We have found that the high frequency surges, due to cold electron emission and sudden discharges in the tube are very feeble in a multi-section tube at 200,000 volts per section, compared with the surges occurring in a single section tube at 500,000 or 700,000 volts. The elimination of inductive connectors in the case of a multi-section tube would therefore probably not place the transformer insulation in danger from the standpoint of surges from the tube, and would allow the tube to be placed closer to the transformer.

The author wishes to express his appreciation to the Rackham Endowment Fund for the financial support of this project, to Professor H. M. Randall, under whose direction this work was begun and carried to completion, to Messrs. D. S. Bayley, E. R. Gaerttner and J. J. Turin, who assisted throughout the work, and to Mr. H. R. Roemer who, as head of the physics department machine shops, deserves a large share of the credit for the successful completion of the apparatus.

Magnetic Interaction and Resultant Anisotropy in Unstrained Ferromagnetic Crystals

L. W. McKeehan
Sloane Physics Laboratory, Yale University, New Haven, Connecticut
(Received May 5, 1937)

The mutual potential energy of two equal and parallel magnets is derived for several especially symmetrical distributions of magnetic moment in each. If R is the distance between magnet centers the first three terms in order of importance depend upon R^{-3}, R^{-5} and R^{-7}. These may be called "dipole," "quadrupole" and "sextupole" terms, respectively. Magnets previously considered as representing the atoms in a ferromagnetic crystal are special cases of one of the general cases here treated. Sextupole terms have not heretofore been included. The distributions of magnetic moment now dealt with permit a closer correspondence between the model magnet in iron, cobalt, and nickel and the probable distribution in these atoms of the electrons responsible for ferromagnetism.

In order to compute ferromagnetic anisotropy—differences in potential energy for differences in direction of magnetization in a crystal—sums of zonal harmonics over the points occupied by atoms are also needed. Such sums for second and fourth-order harmonics have previously been reported for the crystal structures of interest. Sums of sixth-order harmonics are now given.

Within the space assigned in current pictures of the atom to "ferromagnetic" electrons we find ample room for distributions of magnetic moment, agreeing in total amount with observed saturation values, to account in general for reported anisotropies in iron, cobalt, nickel and their cubic alloys. These distributions seem to depend principally upon the maximum number of codirected electron spins. Reported changes of anisotropy with rise of temperature are such as would result from relative rotations of atomic axes out of exact parallelism.

The effects of magnetostrictive strain, here omitted from consideration, may explain some discrepancies in the sign or magnitude of the sextupole terms. In hexagonal cobalt it must be assumed that the molecular field itself is anisotropic.

I. Elementary Magnets

We first consider the mutual potential energy, $2U$, of a pair of equal and parallel magnets each of magnetic moment $\mathbf{P}$ and separated by a distance $\mathbf{R}$. In order to distinguish numerical factors from those involving physical dimensions and units we put $\mathbf{P}=P\mathbf{p}$, where $\mathbf{p}$ is a unit vector, and $\mathbf{R}=ar\mathbf{r}$, where $\mathbf{r}$ is a unit vector and a is the length chosen as a unit. (When we deal with crystals a will be the length of one edge of the unit cell.) This makes r a pure number, the values of which depend only upon the symmetry of the crystal.

The simplest possible magnet is a dipole, anything more complicated than this involves some spatial distribution of magnetic moment and may be called a multipole.

Dipole magnets

The mutual potential energy per magnet can be expressed in closed form if the magnets are simple dipoles. It is

$$U_2=-(P^2/a^3)r^{-3}\mathrm{P}_2\{\cos(\mathbf{p},\mathbf{r})\}. \qquad (1)$$

Here $\mathrm{P}_2\{u\}$ is the second-order zonal surface harmonic, argument u.

Multipole magnets

For magnets more complicated than simple dipoles the mutual potential energy per magnet must be expanded in series form. One such form is

$$U=-(P^2/a^3)\sum_{n=2}^{n=\infty} r^{-n-1}\mathrm{f}_n(\mathbf{p}_a,\ \mathbf{p}_b,\ \cdots\ \mathbf{p}_k,\ \mathbf{r}), \qquad (2)$$

wherein the structure of the multipole fixes the number and the directions of the unit vectors $\mathbf{p}_a$ to $\mathbf{p}_k$, and the form of the numerical functions f_n. There is no term for $n<2$ because the magnets are supposed to have no net magnetic charges.

In (2) the magnets are much more generalized than necessary. If we make all the characteristic directions $\mathbf{p}_a$ to $\mathbf{p}_k$ parallel to a single direction $\mathbf{p}$, and make the structure as symmetrical as possible about a plane perpendicular to $\mathbf{p}$ through its center, the magnet is still complicated enough for practical purposes. It is now what Kornfeld[1] called a zonal multipole and the f_n can be written $F_n\mathrm{P}_n\{\cos(\mathbf{p},\mathbf{r})\}$, F_n being independent of $\mathbf{p}$ and $\mathbf{r}$, so that (2) becomes

[1] H. Kornfeld, Zeits. f. Physik **22**, 27–43 (1924).

$$U_{zm}=-(P^2/a^3)[F_2r^{-3}\mathrm{P}_2\{\cos(\mathbf{p},\mathbf{r})\}+F_4r^{-5}\mathrm{P}_4\{\cos(\mathbf{p},\mathbf{r})\}+F_6r^{-7}\mathrm{P}_6\{\cos(\mathbf{p},\mathbf{r})\}+\cdots]. \quad (3)$$

Upon discovering that $F_2=1$ in all cases we recognize the first term as the dipole energy, (1). By analogy it is customary to call the second term the quadrupole energy, the third term the sextupole energy, and so on. Going still farther some authors proceed to define a "quadrupole moment," "sextupole moment," and so on. The definitions proposed by Kornfeld,[1] and used by Akulov,[2] correspond to the following rearrangement of (3), the terms in braces being the *squares* of the successive moments.

$$U_{zm}=-\{P^2F_2\}(ar)^{-3}\mathrm{P}_2\{\cos(\mathbf{p},\mathbf{r})\}+3\left\{-\frac{P^2F_4a^2}{3}\right\}(ar)^{-5}\mathrm{P}_4\{\cos(\mathbf{p},\mathbf{r})\}$$
$$-10\left\{\frac{P^2F_6a^4}{10}\right\}(ar)^{-7}\mathrm{P}_6\{\cos(\mathbf{p},\mathbf{r})\}+\cdots-(-1)^{\frac{1}{2}n+1}\frac{(n-1)!}{(n/2)!(n/2-1)!}$$
$$\times\left\{(-1)^{\frac{1}{2}n+1}\frac{(n/2)!(n/2-1)!}{(n-1)!}P^2F_na^{n-2}\right\}(ar)^{-n-1}\mathrm{P}_n\{\cos(\mathbf{p},\mathbf{r})\}\cdots. \quad (4)$$

These higher moments are of little or no physical importance, since magnets cannot be constructed which have, let us say, quadrupole moment with no dipole moment. Their definitions also ensure that some of them will be imaginary, e.g., the quadrupole moment of nickel.

Magnetic form factors (F_4, F_6)

In our further analysis we will need F_4 and F_6 for elementary magnets appropriate to atoms of iron, cobalt and nickel. ($F_2=1$ for all models.) The method of deriving the F_n is as follows. Distribute the proposed magnetic moment of one atom, P, consistently with the symmetry already explained, so that the magnetic moment per unit volume is known at all points where it is not zero. Choose a point on the axis of this multipole, well outside its limits. The magnetic field at this point lies along the axis, and can be expressed as a series in ascending negative powers of the distance of the point from the center of the multipole. The potential energy of a dipole with axis parallel to the multipole axis, placed at the point in question, is minus the product of its magnetic moment by the field intensity. The potential energy for nonaxial positions of the dipole is derived from the series thus found by multiplying each term by the appropriate zonal surface harmonic.

Now suppose a second multipole like the first (or of some other type, in case of alloys) and with its axis parallel to that of the first. Place the center of the second multipole on the axis of the first at such a distance that their magnetic structures do not overlap. The mutual potential energy is found by integrating the expression for the energy per unit magnetic moment, already found as a function of distance and polar angle, over points where the magnetic moment of the second multipole differs from zero. Under the given conditions the series thus obtained converges. Arrange it in ascending negative powers of the single coordinate defining the relative positions of the two structures.

Again extend the result to three dimensions by introducing zonal surface harmonics of appropriate orders. The coefficients of the zonal harmonics in this series are the required F_n.

We are interested in distributions of magnetic moment suggested by, or at least consistent with, spectroscopic data. Slater[3] gives tables from which we can conclude that the $3d$ electrons supposed to account for the unbalanced magnetic moment in iron, cobalt, and nickel are concentrated at a distance from the nucleus which can be estimated in each of these elements and which does not vary greatly in this triad. Let us call this distance ρa, expressed as a numerical multiple of the unit length a. We will find the F_n for a few simple structures.

Case 1. Sphere (spherical shell)

It appears without detailed analysis that all distributions of magnetic moment which have

[2] N. S. Akulov, Zeits. f. Physik **57**, 249–256 (1929).
[3] J. C. Slater, Phys. Rev. **36**, 57–64 (1930).

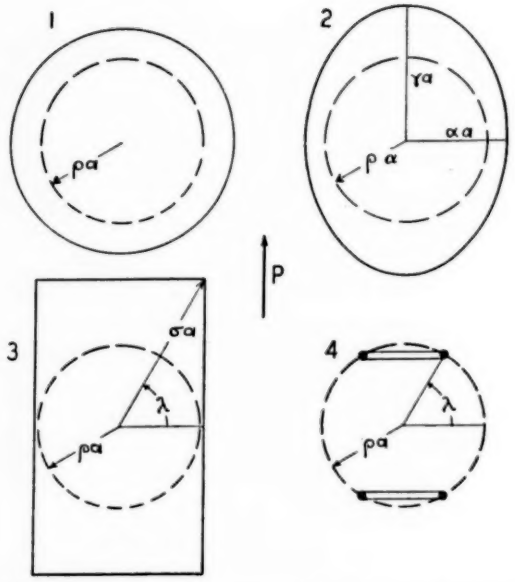

FIG. 1. Cross sections of magnetic elements. (See Table I.)

spherical symmetry, except for the fact that all the elementary volumes have parallel magnetic axes, have $F_n=0$ for $n>2$. Such structures are therefore equivalent to dipoles. This means that our analysis is not really restricted, as it seemed to be, to swarms of point electrons. Spatially extensive electrons, so long as the magnetic moment per unit volume in each is a function only of the radius, give the same results.

Case 2. Spheroid (spheroidal shell)

The next simplest case is that of a uniformly magnetized spheroidal magnet, a spheroid filled with uniform volume distribution of magnetic moment. Symmetry requires the magnetic axis to be the axis of figure. Fig. 1 shows a cross section of such a spheroid, the corresponding ρa being shown as a broken circle within the spheroid of semiaxes αa, αa, γa. Table I gives expressions for F_4 and F_6 in terms of α and γ. It will be noticed that when $\gamma=\alpha$, F_4 and F_6 vanish as they should for a sphere.

Since F_4 and F_6 depend only upon $(\gamma^2-\alpha^2)$, which is the same for all confocal ellipses, it is clear that spheroidal shells and distributions built up by superposing such shells have constant F_4 and F_6 so long as all shells are defined by the same focal points. Notice that prolate spheroids have positive F_4, oblate spheroids negative F_4, but that F_6 can only be positive in either case. The ratio of ρa to γa and αa involves elliptic integrals.

Case 3. Cylinder

A more conventional shape of magnet is a right circular cylinder, uniformly magnetized along its axis, and this is the only model hitherto considered in magnetic interaction studies. Fig. 1 suggests how the length ($\sigma a \sin\lambda$) and radius ($\sigma a \cos\lambda$) of such a cylinder are related to the mean radial distance ρa of its volume elements from its center. The actual relation is very complicated. Table I shows how F_4 and F_6 depend upon the shape and size of the cylinder.

The expressions for F_4 at the limits, $\lambda=0$ and $\lambda=\pi/2$, that is for a circular current loop and for an infinitely thin bar magnet, have been known for many years.

Case 4. Pair of dicircles

None of the structures so far discussed seems suitable for a first approximation to actual atomic magnets. The dependence of ρa upon limiting dimensions of the model structure is highly inconvenient, and unduly increases the labor of computation. There is only one way to avoid this difficulty, by keeping all the magnetic moment on a sphere of radius ρa. Symmetry requires that the simplest general model of this type have its magnetic moment spread uniformly along two parallels of latitude, at $+\lambda$ and $-\lambda$. Each of these circles may be called a dicircle (analogous to dipole). It is easy to see that the limiting cases, $\lambda=0$ and $\lambda=\pi/2$, must give the extreme possible values of F_4 for any distribution not extending beyond ρa. Table I shows that this case, like case 3, permits both positive and negative F_6.

The restriction to zonal multipoles is not as artificial as it seems, for unless the symmetry of the model atom about the axis of magnetization is equal to or higher than the symmetry of the crystal about the same axis the analysis becomes unmanageable. Since the axis of magnetization is to be unrestricted this means that it must tolerate both four fold and threefold rotations in cubic crystals, that is, it must have complete rotational symmetry. If a physical basis is

TABLE I. *Magnetic form factors, F_4 and F_6. (See Fig. 1 for definition of symbols.)*

Case 1. Sphere
$F_4=0$; $F_6=0$.
Case 2. Spheroid
$F_4=12(\gamma^2-\alpha^2)/5$; $F_6=216(\gamma^2-\alpha^2)^2/35$.
Case 3. Right circular cylinder
$F_4=\sigma^2(4-7\cos^2\lambda)$;
$F_6=\sigma^4(128-496\cos^2\lambda+443\cos^4\lambda)/8$,
$F_4=0$ for $\lambda=\pm40°-54'$;
$F_6=0$ for $\lambda=\pm32°-11'$, $\pm50°-34'$.
Maxima: $F_4=4\sigma^2$; $F_6=16\sigma^4$, $75\sigma^4/8$.
Minima: $F_4=-3\sigma^2$; $F_6=-600\sigma^4/443$ for $\lambda=\pm41°-34'$.
Case 4. Pair of dicircles
$F_4=6\rho^2(2-3\cos^2\lambda)$;
$F_6=15\rho^4(32-112\cos^2\lambda+89\cos^4\lambda)/4$.
$F_4=0$ for $\lambda=\pm35°-16'$;
$F_6=0$ for $\lambda=\pm25°-07'$, $\pm48°-32'$.
Maxima: $F_4=12\rho^2$; $F_6=120\rho^4$, $135\rho^4/4$.
Minima: $F_4=-6\rho^2$;
$F_6=-1080\,\rho^4/89$ for $\lambda=\pm37°-31'$.

desired, the model may be thought of as representing the average aspect of a rigid group of electrons with random azimuths in the different atoms of the crystal.

II. FERROMAGNETIC CRYSTALS

Magnetic potential energy density

In an infinite crystal with N zonal multipoles per unit cell of volume V the mean magnetic potential energy density is

$$E=(N/V)\sum' U_{zm}, \qquad (5)$$

where the primed summation is to be taken for all pairs of magnets which have one selected magnet in common. (If all the magnets are not alike, or if their environments differ, the selected magnets must include all sorts in proper proportions, and a suitable mean value of E is to be found; see Alloys, below.)

In perfect crystals the indicated summations can be effected to any desired precision. In actual imperfect crystals these ideal values will be more or less departed from. Previous work[4] has shown that results of computation will be comparable with experiment in crystals where the atoms at small r lie nearly at the points of a perfect lattice with a point at the origin atom, and where there is no systematic deviation from perfect arrangement (no elastic strain).

[4] L. W. McKeehan, Phys. Rev. **43**, 913–923, 924–930, 1022–1024, 1025–1029; **44**, 38–42, 582–584 (1933)

Collecting common factors and using the abbreviation, $S_n=\sum' r^{-n-1}P_n\{\cos(\mathbf{p},\mathbf{r})\}$, we rewrite (5) in the form

$$E=-(NP^2/Va^3)[F_2S_2+F_4S_4+F_6S_6+\ldots]. \qquad (6)$$

The volume of the unit cell can be expressed in terms of the parameter a and axial ratios. In cubic crystals the edges of the unit cube being each equal to a, we have $V=a^3$. In hexagonal crystals the edges of the unit prism are a, a and ca, the first two being 120° apart and the third (principal) axis perpendicular to these, so that $V=a^3c\sqrt{3}/2$.

We need S_2, S_4 and S_6 for body-centered and face-centered cubic lattices and for hexagonal close-packing. It involves no extra work to get these sums for simple cubic and simple hexagonal lattices (primitive lattices) as well.

Lattice sums—dipole terms

In finding S_2 we must specify boundary conditions, because an important part of S_2 (in cubic crystals all of it) depends upon magnets lying outside a large sphere centered at the origin and wholly inside the actual boundary of the specimen. The least special boundary to choose is one at infinity, and this is essentially what we do when we use the rapidly convergent series forms given in Appendix I. Finite boundaries equivalent at the origin to a boundary at infinity are those for which the so-called demagnetizing field is zero. This means that experimental results, corrected for demagnetizing fields, as they usually are, may be compared directly with our calculations, presented in Table II.

TABLE II. *Coefficients in zonal harmonic lattice sums S_2, S_4, and S_6.*

	Atomic Arrangement				
	Cubic			Hexagonal, $c=2\sqrt{6/3}$	
Coefficient	Primitive	Body-Centered	Face-Centered	Primitive	Close-Packed
S_2	2.09440	4.18879	8.37758		
S_{20}				2.75741	2.96023
S_{22}				−3.82936	0.00507
S_{40}	3.10823	−3.10734	−7.19838	0.95461	0.33815
S_{60}	0.57333	5.44656	−26.63489		
S_{62}				−1.91857	−4.15924
S_{66}				2.66930	2.51851

In cubic crystals S_2 does not depend upon the direction (**p**) of the magnetization. The series form (Appendix I) is not needed here, since $S_2=2\pi N/3$ in all cases.

In hexagonal crystals

$$S_2=S_{20}+S_{22}p_3^2. \quad (7)$$

Here p_3 is the component of **p** along the hexagonal axis. The series in Appendix I contain a general axial ratio, c, but only a particular value of $c=2\sqrt{6}/3$ has been used in computing S_{20} and S_{22} for Table II. This is the axial ratio for hexagonal close-packing of spheres. It differs a little from the axial ratio in hexagonal cobalt, $c=1.624$, but is much more convenient, since many values of r^2 are integers when $c=2\sqrt{6}/3$. Table II does not show what part of S_{20} depends upon remote magnets. This may be computed directly as $4\pi N\sqrt{3}/9c$. For the two arrangements chosen $N=1, 4\pi N\sqrt{3}/9c=1.48096$, and $N=2, 4\pi N\sqrt{3}/9c=2.96192$. It will be noticed that in hexagonal close-packing nearby magnets contribute very little to S_{20}.

Lattice sums—quadrupole terms

The sum S_4 converges absolutely, that is, it does not depend appreciably upon remote magnets. In cubic crystals

$$S_4=S_{40}\{1-5(p_2^2p_3^2+p_3^2p_1^2+p_1^2p_2^2)\}, \quad (8)$$

wherein p_1, p_2, p_3 are the direction-cosines of **p** with respect to the cubic axes.

In hexagonal crystals

$$S_4=S_{40}\{1-10p_3^2+(35/3)p_3^4\}. \quad (9)$$

This may also be written

$$S_4=(8S_{40}/3)\,\mathrm{P}_4\{p_3\}. \quad (10)$$

Lattice sums—sextupole terms

Though S_6 converges more rapidly than S_4 its convergence is still so slow that the special forms in Appendix I must be used if precision is desired. In cubic crystals

$$S_6=S_{60}\{1-(21/2)(p_2^2p_3^2+p_3^2p_1^2+p_1^2p_2^2)+(231/2)p_1^2p_2^2p_3^2\}. \quad (11)$$

In hexagonal crystals a rectangular frame of reference is inappropriate, since it conceals the true symmetry of the functions of direction. We therefore define **p** by θ_3, the angle it makes with the hexagonal axis, and by the azimuth, ϕ, of the plane through **p** and the hexagonal axis, measured from the nearest prism face of form {100}. In terms of these coordinates

$$S_6=S_{63}\mathrm{P}_6\{\cos\theta_3\}+S_{66}\cos 6\phi\,\sin^6\theta_3. \quad (12)$$

III. Comparison Between Theory and Experiment

There is already a considerable amount of information about ferromagnetic anisotropy, especially regarding iron, cobalt, nickel and their alloys.[5] The best way of presenting the experimental findings is to give the values of coefficients appearing in an empirical equation for the magnetic potential energy density as a function of the direction of magnetization. In cubic crystals this is

$$E=K_0+K_1(p_2^2p_3^2+p_3^2p_1^2+p_1^2p_2^2)+K_2p_1^2p_2^2p_3^2. \quad (13)$$

In hexagonal crystals the analogous equation is, to the same degree,

$$E=K_0+H_1\cos^2\theta_3+H_2\cos^4\theta_3+H_3\cos^6\theta_3+H_4\cos^6\phi\,\sin^6\theta_3. \quad (14)$$

The way in which K_1 and K_2, in (13), can be derived from experimental data of various kinds has been described by Bozorth.[6] No attempt has yet been made to evaluate all the possible coefficients appearing in (14). The constant term in (13) and (14), K_0, cannot be found by experiment and is of slight interest, anyway, since it is completely negligible in comparison with the potential energy decrease arising from non-magnetic interaction (the molecular field). The forms of (13) and (14) depend only upon crystalline symmetry, though (13) may be written in various ways by using the identity: $p_1^2+p_2^2+p_3^2=1$.

Among various ways of fitting model magnets to the experiments the one here chosen is to select an extreme model of plausible type for each of the atoms present, to compute the coefficients in (13) or (14) consistent with these

[5] For a recent compilation of results see L. W. McKeehan, Phys. Rev. **51**, 136–139 (1937). This should be consulted for the sources of data concerning cubic metals and alloys.

[6] R. M. Bozorth, Phys. Rev. **50**, 1076–1081 (1936).

model atoms in the actual crystal structure and to compare these computed values with available experimental values. If the computed coefficients are too large we can get a better fit by reducing the dimensions of the model magnet, or by allowing for heat motions and other displacements from ideal arrangements. If the computed coefficients are too small or are of the wrong sign we must admit other causes for anisotropy than those discussed above. One such cause may be given special mention at this point.

Effects of homogeneous strain

It is well known that elastic strains may be large enough to confer extra stability on one of the preferred directions for magnetization in a cubic crystal (directions for minimum E) and may even make magnetization easiest along a direction not preferred in the unstrained crystal.[7] The lattice sums S_2, in our notation, become dependent upon the direction of magnetization, **p**, even in crystals originally cubic. They depend also upon the strain tensor. The magnetostrain may be considered[8] as that self-imposed strain which makes the total potential energy—magnetic and elastic—minimal. Our computation of E has ignored these effects upon S_2 and is therefore certain to be inexact. The sums S_4 will also be affected by strain, though less seriously, because the strain does not here upset an exact balance as it does when $S_2=0$ in the unstrained crystal.

The reason for ignoring the effects of strain in this first approximation is that the strain argument gives the wrong sign for the magnetostriction of nickel,[8] and cannot therefore be as important as was first supposed. The extreme smallness of magnetostrains in comparison with elastic strains known to alter preferred directions for magnetization also means that something else than strain must explain the relatively large differences in E for different directions in well-annealed crystals.

The idea at the bottom of the present analysis, that the shape of the atomic magnet principally accounts for preferred orientations of these magnets in crystals, is not of recent origin. What is new is the suggestion[9] that the appropriate shape differs in different atoms, particularly in iron and in nickel.

Theoretical anisotropy

In cubic crystals we find by comparing (6) with (13) that

$$K_0=-(NP^2/Va^3)\times[F_2S_2+F_4S_{40}+F_6F_{60}+\dots], \quad (15)$$

$$K_1=-(NP^2/Va^3)\times[-5F_4S_{40}-(21/2)F_6S_{60}+\dots], \quad (16)$$

$$K_2=-(NP^2/Va^3)[(231/2)F_6S_{60}+\dots]. \quad (17)$$

In hexagonal crystals we will compare values of E for three important directions: the hexagonal axis, [001]; a close-packed line and twofold axis in the basal plane, [100]; one of the other set of twofold axes in the basal plane, [210]. For these directions we find

$$E_{001}=-(NP^2/Va^3)[F_2S_{20}+F_2S_{22}+(8/3)F_4S_{40}+F_6S_{63}+\dots], \quad (18)$$

$$E_{100}=-(NP^2/Va^3)[F_2S_{20}+F_4S_{40}-(5/16)F_6S_{63}+F_6S_{66}+\dots], \quad (19)$$

$$E_{210}=-(NP^2/Va^3)[F_2S_{20}+F_4S_{40}-(5/16)F_6S_{63}-F_6S_{66}+\dots]. \quad (20)$$

For reasons already given we confine ourselves to dicircle models, case 4 of Fig. 1 and Table I. Data used in computation are collected in Table III.

Pure metals (Table III)

Iron (body-centered cubic).—We put $\lambda=0$ for an equatorial concentration of magnetic moment in iron. That this is necessary was first clearly stated by Mahajani.[10] It is consistent with the large number, four, of disposable spins in iron, since not more than two electrons could occupy the other extreme position, $\lambda=\pi/2$, without interference. We reject the most symmetrical arrangement of four points—in a regular tetrahedron with two of its edges perpendicular to the magnetic axis—because this puts dicircles at $\lambda=\pm35°-16'$, making $F_4=0$, F_6 negative, so that K_1 becomes negative, contrary to experi-

[7] R. Becker, Zeits. f. Physik **62**, 253–269 (1930); F. Bitter, Phys. Rev. **42**, 697–708 (1932).
[8] N. S. Akulov, Zeits. f. Physik **52**, 389–405 (1928).
[9] R. M. Bozorth, L. W. McKeehan, Phys. Rev. **51**, 216 (1937).
[10] G. S. Mahajani, Proc. Camb. Phil. Soc. **23**, 136–143 (1926); especially footnote on page 138.

ence. Furthermore, the average number of unbalanced spins per atom lies between two and three so that the existence of four in one atom cannot be typical.

With this assignment of λ we find $K_1=25.46\times10^6$ erg. cm^{-3}, $K_2=-167.1\times10^6$ erg. cm^{-3}. (Hereafter we suppress the constant factor 10^6 erg. cm^{-3} in E and its parts.) As far as K_1 is concerned a smaller or less extremely equatorial structure would be better, since the experimental value of K_1 at room temperature is only 0.42. The sign of K_2 is wrong and it is about one thousand times greater than necessary. It remains to be seen whether this discrepancy in sign can be accounted for by magnetostriction. The persistence of relatively high K_2 right up to the temperature (600°C) at which K_1 reaches a very low value is in favor of the dependence of K_2 on some factor which does not change as rapidly with temperature as we expect sextupole magnetic interaction to change.

Nickel (*face-centered cubic*).—Having selected

TABLE III. *Calculated anisotropy of pure metals.*

Part 1. Cubic crystals

ELEMENT		Fe	(Fe)	Co	(Co)	Ni	(Ni)
Magnetic moment per atom*	$P\times10^{20}$	2.055	2.055	1.5794	1.5794	0.5883	0.5883
Atomic weight	A	55.85	55.84	58.94	58.94	58.69	58.69
Diameter of 3*d* shell**	$2\rho a$	1.53	1.53	1.38	1.38	1.27	1.27
Crystal structure		B.C.C.	F.C.C.	F.C.C.	B.C.C.	F.C.C.	B.C.C.
Number of atoms per cell	N	2	4	4	2	4	2
Lattice parameter***	$a\times10^8$	2.861	3.646	3.545	2.846	3.517	3.00
Relative radius of 3*d* shell	ρ	0.267	0.210	0.195	0.242	0.181	0.212
Latitude of dicircles	λ	0	0	$\pi/2$	$\pi/2$	$\pi/2$	$\pi/2$
Magnetic form factors							
Quadrupole factor	F_4	−0.4290	−0.2641	0.4546	0.7054	0.3912	0.5376
Sextupole factor	F_6	0.1725	0.0654	0.1722	0.4146	0.1275	0.2409
Anisotropy coefficients							
First (quadrupole part)		10.26	6.84	−8.23	−10.29	−1.03	−0.79
First (sextupole part)		15.20	−13.16	−24.21	22.26	−2.61	1.31
First (total)	K_1	25.46	−6.32	−32.44	11.97	−3.64	0.52
Second (sextupole)	K_2	−167.1	144.7	266.4	−244.9	28.7	−14.4

Part 2. Hexagonal cobalt

Magnetic moment per atom*	$P\times10^{20}$	1.5794	
Atomic weight	A	58.94	
Diameter of 3*d* shell**	$2\rho a$	1.38	
Crystal structure		H.C.P.	
Number of atoms per cell	N	2	
Lattice parameter***	a	2.507	
Axial ratio—observed		1.624	
Axial ratio—assumed	$2\sqrt{6}/3$	1.633	
Relative raidus of 3*d* shell	ρ	0.275	
Latitude of dicircles	λ	0	$\pi/2$
Magnetic form factors			
Quadrupole factor	F_4	−0.4545	0.9090
Sextupole factor	F_6	0.1937	0.6886
Energy density differences			
$E_{100}-E_{001}$			
Dipole part		0.0072	0.0072
Quadrupole part		0.7279	−0.3640
Sextupole part		−5.5878	−1.5716
Total		−4.8527	−1.9284
$E_{210}-E_{001}$			
Sextupole part		−5.0949	−1.4330
Total		−4.3598	−1.7898
$E_{210}-E_{100}$			
(Sextupole) total		0.4929	0.1386

* Values for Fe and Ni based on M. Fallot, *Dissertation* (Strasbourg, 1935). Magnetic moment per gram-atom, $\sigma_0=221.74$ for Fe, $\sigma_0=60.41$ for Ni; $P=\sigma_0 A/N_0$ with $N_0=6.026\times10^{23}$ atoms per gram-atom. Value for Co based on R. I. Allen, F. W. Constant, Phys. Rev. **44**, 228–233 (1933). Saturation magneization $I_{sat}=1418$, $P=I_{sat}/Na^3$.

** J. C. Slater, Phys. Rev. **36**, 57–64 (1930), column (5), Table I(*d*), p. 62.

*** Values for stable metals and F.C.C. cobalt from M. C. Neuburger, Zeits. f. Krist. **93**, 1–36 (1936).

$\lambda=0$ for iron we put $\lambda=\pi/2$ for nickel, noticing that this is the best of all possible choices for a pair of disposable spins. In this case we have unique data at very low temperatures,[11] so that our model should receive its severest test. We compute $K_1=-3.64$; $K_2=28.7$ and can derive from the published curves the following values for comparison at $-252.3°$: $K_1=-2.8$, $K_2=4.2$. The experimental values are rendered rather uncertain by the fact that saturation was attained only along [111] at the lowest temperature, so that extensive extrapolations were necessary in finding K_1 and K_2. The agreement is very gratifying.

Cobalt (hexagonal close-packed).—In this crystal structure there is some preference for axial magnetization due merely to dipole terms. But the whole difference in energy in favor of axial magnetization[12] is much too large to be accounted for by dipole terms alone. At $-190°$C we find $E_{100}-E_{001}=8.81$, $E_{210}-E_{001}=9.44$, and the part due in each of these to dipole interactions is only 0.0072 for the axial ratio $c=2\sqrt{6}/3=1.633$. Shrinking the axial ratio to its experimental value, $c=1.624$, increases the dipole coefficient S_{22} from 0.00507 to 0.03497 and correspondingly raises $E_{100}-E_{001}$ and $E_{210}-E_{001}$ to 0.0500 which is still far too low.[13] It is therefore necessary to look for higher order terms of proper sign. The first guess, since the number of disposable spins is greater than two, is to put $\lambda=0$. If we consider only the quadrupole terms in addition to dipole terms, we find for $\lambda=0$, $E_{100}-E_{001}=E_{210}-E_{001}=0.735$, which is still inadequate in amount and, moreover, leaves the experimental finding $E_{210}-E_{100}=0.63$ unaccounted for. The last defect is remedied by including the sextupole terms. These yield $E_{210}-E_{100}=0.493$, in reasonable agreement with what seems to be needed. The differences $E_{100}-E_{001}$ and $E_{210}-E_{001}$ change sign, however, so that the principal problem, to explain the high stability for axial magnetization, is farther from solution than before.

If we try $\lambda=\pi/2$, which is not impossible since the average number of unbalanced spins per atom is here less than two, the sextupole terms account for $E_{210}-E_{100}=0.138$, which is hardly enough. The computed values of $E_{100}-E_{001}$ and $E_{210}-E_{100}$ are again of the wrong sign, though not so negative as for $\lambda=0$. The quadrupole terms now contribute to the anomaly and this is a clue to a possible choice between $\lambda=0$ and $\lambda=\pi/2$, for above 260°C the experiments[12] show that the hexagonal axis is avoided rather than preferred. The relative importance of quadrupole terms, as compared with sextupole terms, should of course be greater at higher temperatures.

We suggest as the best way out that the low temperature preference for the hexagonal axis must have a nonmagnetic origin. This amounts to saying that electrostatic interactions are responsible, or that the molecular field has a maximum along the hexagonal axis at low temperatures, and that this maximum decreases rapidly as the temperature rises so that above 260°C the magnetic interactions, now mainly of quadrupole order, predominate. For the magnetic interactions we therefore propose $\lambda=\pi/2$ as the best first approximation.

Unstable forms

Face-centered cubic cobalt can be preserved at room temperature by quenching from temperatures at which it is the stable form. The metal is ferromagnetic in both modifications and has about the same saturation magnetization.[14] The ferromagnetic anisotropy of the cubic arrangement has not been studied experimentally. We include in Table III predictions of its anisotropy constants at low temperatures (total K_1, K_2) and at higher temperatures (quadrupole part of K_1). The anisotropy of body-centered cubic nickel and cobalt (neither of these is known to exist) and that of face-centered cubic iron (not known as a pure metal) have also been computed. In these cases it has been necessary to estimate

[11] K. Honda, H. Masumoto, Y. Shirakawa, Sci. Rep. Tohoku Imp. Univ. **24**, 391–410 (1935).

[12] S. Kaya, Sci, Rep. Tohoku Imp. Univ. **17**, 1157–1177 (1928); K. Honda, H. Masumoto, Sci. Rep. Tohoku Imp. Univ. **20**, 323–341 (1931): for energy differences based on these experiments see L. W. McKeehan, Trans. A. I. M. E. **111**, 11–52 (1934), especially Table 3, p. 47.

[13] The effect of small changes in c has been discussed in a previous paper, L. W. McKeehan, Phys. Rev. **43**, 1025–1029 (1933). In using the formulae there given notice that the present S_2 is $-u/2$ in the earlier notation.

[14] R. I. Allen, F. W. Constant, Phys. Rev. **44**, 228–233 (1933).

lattice parameters by extrapolating the parameter-concentration curves of appropriate alloy series, and to assume that the magnetic moment per atom remains the same as in the forms stable at low temperatures. Neither of these procedures is justified. In all these cases the value of λ chosen for the low temperature form has been used throughout.

Alloys (Table IV)

We can now proceed to compute anisotropies in alloys of iron, cobalt, and nickel. We postulate that the magnetic form factors found most suitable for the pure metals are unaltered by mixture. Two types of alloy will be considered. In the solid solution type the distribution of the component atoms over the occupied points is entirely at random. In the perfectly ordered, or superstructure type, the distribution of each component has the full symmetry of the space lattice. This restricts the composition to definite proportions, different in superstructures derived from solid solutions with different space lattices. There is no difficulty, in principle, in dealing with intermediate cases, partial order in compositions consistent with perfect order, or in compositions differing from these, where perfect order is impossible. Such intermediate cases are merely more cumbersome to formulate and compute.

Solid solutions

In Eq. (6) we need to use instead of P^2F_2, P^2F_4 and P^2F_6 suitable mean values of these quantities. Let the fractions of the nickel, iron, and cobalt nickel be, respectively, f_A, f_B, f_C, and let their magnetic moments per atom be P_A, P_B, P_C. There will be form factors, F_{4A}, F_{6A} and others corresponding to pairs of like atoms, already given in Table III, and new factors, F_{4AB}, F_{6AB}, and others, corresponding to pairs of unlike atoms. With $\lambda_B=0$, $\lambda_A=\lambda_C=\pi/2$ we have the following cross factors:

$$
\begin{aligned}
F_{4BC}&=-3\rho_B^2+6\rho_C^2,\\
F_{4CA}&=6\rho_C^2+6\rho_A^2,\\
F_{4AB}&=6\rho_A^2-3\rho_B^2,\\
F_{6BC}&=(45/8)\rho_B^4-45\rho_B^2\rho_C^2+40\rho_C^4,\\
F_{6CA}&=15\rho_C^4+90\rho_C^2\rho_A^2+15\rho_A^4,\\
F_{6AB}&=40\rho_A^4-45\rho_A^2\rho_B^2+(45/8)\rho_B^4.
\end{aligned}
$$

As an example, we have for a ternary solid solution,

$$
\begin{aligned}
\overline{P^2F_4}=&f_A^2P_A^2F_{4A}+2f_Af_BP_AP_BF_{4AB}\\
&+2f_B^2P_B^2F_{4B}+2f_Bf_CP_BP_CF_{4BC}\\
&+f_C^2P_C^2F_{4C}+2f_Cf_AP_CP_AF_{4CA}. \qquad (21)
\end{aligned}
$$

Formulae like this have been used to get the values of K_1 and K_2 in Table IV for several series of solid solutions.

Superstructures

In a superstructure alloy the two or more kinds of atom present do not have, even on the average, the same environments, so that in finding the mean energy density we have to include the lattice sums among the variable factors. The only exception to this occurs in cubic structures, the mean environment of each species of atom continuing to possess cubic symmetry so that S_2 still vanishes separately for each species. One formula for a binary alloy will be expanded as an example of what has to be done.

$$
\begin{aligned}
\overline{P^2F_4S_{40}}=&f_A\bar{S}_{40AA}P_A^2F_{4A}\\
&+(f_A\bar{S}_{40AB}+f_B\bar{S}_{40BA})P_AP_BF_{4AB}\\
&+f_B\bar{S}_{40BB}P_B^2F_{4B}. \qquad (22)
\end{aligned}
$$

Here $\bar{S}_{4AA}$ is the mean lattice sum of the fourth order zonal harmonic over those points surrounding an atom of component A which are also occupied by A atoms. This mean is found by considering in turn the various A atoms in the unit cell as origin. Similarly $\bar{S}_{40AB}$ is the mean sum over those points surrounding an A atom which are occupied by B atoms. Notice that $\bar{S}_{40BA}$ is not necessarily the same as $\bar{S}_{40AB}$.

Binary alloys

Iron-cobalt (body-centered cubic).—In computing K_1 and K_2 for iron-cobalt alloys we have assumed that the lattice parameter a varies linearly with atomic composition,[15] and that the

[15] A. Osawa, Sci. Rep. Tohoku Imp. Univ. **19**, 109–121 (1930). Values of a for iron and for a 50–50 alloy, from unpublished work of F. E. Haworth, agree closely with Osawa's curve of a-*vs.*-composition.

TABLE IV. *Calculated anisotropy of alloys.*

Part 1. Iron-cobalt—body-centered cubic solid solutions

Iron atomic percent		100	90	80	70	60	50	40	30
Cobalt atomic percent		0	10	20	30	40	50	60	70
Anisotropy coefficients									
First (quadrupole part)		10.26	7.80	5.43	3.14	0.94	−1.16	−3.18	−5.10
First (sextupole part)		15.20	11.27	8.32	6.89	5.47	5.58	6.75	8.98
First (total)	K_1	25.46	19.07	13.75	9.53	6.41	4.42	3.57	3.88
Second (sextupole)	K_2	−167.1	−123.9	−91.6	−70.2	−60.1	−61.4	−74.2	−98.8

Part 2. Iron-nickel—body-centered cubic solid solutions

Iron atomic percent		100	90	80
Nickel atomic percent		0	10	20
Anisotropy coefficients				
First (quadrupole part)		10.26	7.89	5.87
First (sextupole part)		15.20	11.34	8.91
First (total)	K_1	25.46	19.23	14.78
Second (sextupole)	K_2	−167.1	−124.8	−98.0

Part 3. Nickel-iron—face-centered cubic solid solutions

Nickel atomic percent		100	90	80	70	60	50	40	30
Iron atomic percent		0	10	20	30	40	50	60	70
Anisotropy coefficients									
First (quadrupole part)		−1.03	−0.81	−0.43	0.10	0.76	1.54	2.42	3.40
First (sextupole part)		−2.61	−1.71	−1.38	−1.57	−2.21	−3.26	−4.67	−6.40
First (total)	K_1	−3.64	−2.52	−1.81	−1.47	−1.45	−1.72	−2.25	−3.00
Second (sextupole)	K_2	28.7	18.8	15.2	17.2	24.3	35.8	51.4	70.4

Part 4. Nickel-cobalt—face-centered cubic solid solutions

Nickel atomic percent		100	90	80	70	60	50	40	30
Cobalt atomic percent		0	10	20	30	40	50	60	70
Anisotropy coefficients									
First (quadrupole part)		−1.03	−1.45	−1.95	−2.51	−3.14	−3.83	−4.59	−5.41
First (sextupole part)		−2.61	−3.84	−5.29	−6.69	−8.83	−10.91	−13.19	−15.67
First (total)	K_1	−3.64	−5.29	−7.24	−9.47	−11.97	−14.47	−17.78	−21.08
Second (sextupole)	K_2	28.7	42.2	58.2	76.5	97.2	120.0	145.1	172.4

Part 5. Nickel-iron-cobalt—face-centered cubic solid solutions

Nickel atomic percent		50	50	50	50	50	50
Iron atomic percent		50	40	30	20	10	0
Cobalt atomic percent		0	10	20	30	40	50
Anisotropy coefficients							
First (quadrupole part)		1.54	0.39	−0.72	−1.80	−2.84	−3.83
First (sextupole part)		−3.26	−3.60	−3.99	−5.28	−7.56	−10.91
First (total)	K_1	−1.72	−3.21	−4.71	−7.08	−10.40	−14.74
Second (sextupole)	K_2	35.8	39.6	43.9	58.0	83.2	120.0

Part 6. Comparison of solid solutions and superstructure alloys

Composition		FeCo	Ni_3Fe	Ni_3Co
Anisotropy coefficients (solid solution)				
First (quadrupole part)		−1.16	−0.18	−2.22
First (sextupole part)		5.58	−1.42	−6.10
First (total)	K_1	4.42	−1.60	−8.32
Second (sextupole)	K_2	−61.4	15.6	67.0
Anisotropy coefficients (superstructure)				
First (quadrupole part)		−5.26	−1.62	−1.60
First (sextupole part)		−4.73	0.28	−5.28
First (total)	K_1	−9.98	−1.34	−6.88
Second (sextupole)	K_2	52.0	−3.0	58.1

atomic moments are unaltered by mixture. The latter assumption is probably wrong, in view of the high magnetizations possible from 30 Co to 50 Co, but the general picture of what happens is not much altered by mistakes in the magnetic moments (P_B and P_C).

The experimental values of K_1 at room temperature agree fairly well in general trend with the computed values of the quadrupole part of K_1, not at all with total K_1. We conclude that the relative importance of sextupole terms, which account for positive K_1 at high cobalt contents,

is already greatly diminished at this temperature. The transition point from K_1 positive to K_1 negative cannot be brought to a cobalt content of less than 45 atomic percent even by ignoring sextupole terms entirely, so the quantitative agreement is not wholly satisfactory in this respect. The anomalous sign of observed K_2 in iron is replaced by the expected sign at or near the composition for which K_1 passes through zero. The present theory does not offer any explanation of this.

The formation of the possible superstructure in FeCo should reverse the positive sign of K_1, and negative sign of K_2, predicted for very low temperatures in the solid solution. If the quadrupole terms predominate, as we see that they do at room temperature and above, K_1 should merely become more negative, K_2 should still reverse its sign. It would probably be difficult to detect the latter effect because K_2 must be small in comparison with its low temperature limit for either structure.

Iron-nickel (*body-centered cubic*).—A few points have been computed for body-centered iron-nickel alloys. Nothing is known of their ferromagnetic anisotropy and the assumptions of unaltered moment per atom and of linear change of lattice parameter with increase in nickel content are very rough approximations.

Nickel-iron (*face-centered cubic*).—Jette and Foote[16] have shown that the lattice parameter varies linearly over a wide range in the nickel rich nickel-iron alloys but not over quite so wide a range as here assumed. As in body-centered iron-cobalt solutions the change in sign of K_1 actually occurs at a composition (24 percent iron) a little too near the starting point to be accounted for, even by ignoring sextupole terms altogether. Except for this the qualitative agreement as to K_1 is reasonably good. The sign of K_2 disagrees with observation. As in all the alloys and pure metals the observed values of K_2 are extremely small in comparison with calculated values. A possible superstructure (not yet observed to occur) at Ni_3Fe has been investigated. The changes in K_1 and K_2 which should result from the formation of the orderly structure are not very striking.

[16] E. R. Jette, F. Foote, Trans. A. I. M. E. **120**, 259–276 (1936).

Nickel-cobalt (*face-centered cubic*).—This series has been reported[5] to show a positive K_1, over a narrow range near the nickel end. The calculated K_1 is everywhere negative, and the model does not seem to be flexible enough to accommodate itself to a double change in sign of K_1. The rapid descent of K_1 as we approach the cobalt end is in agreement with experiment. We prefer to leave the misfit for further study rather than to devise an *ad hoc* hypothesis to explain it. It may be mentioned, however, that if K_1 does have two zero values on this boundary of the ternary diagram it is very surprising that no magnetically soft nickel-cobalt alloys have been developed.

Ternary alloys

Nickel-iron-cobalt (*face-centered cubic*).—A single cut of the ternary diagram has been made at 50 percent nickel. As expected from the binary alloys, K_1 must be ascribed mainly to quadrupole terms in order to agree qualitatively with the experimental results,[5] of which several lie on this cut.

IV. Conclusion

Most of the minor discrepancies mentioned above could be avoided by using a less extreme type of model, in particular by allowing the dicircle latitude, λ, to have other values than 0 and $\pi/2$. This seemed inadvisable in a first survey of the data, but is actually well justified at temperatures far from absolute zero, for the blurring of exact alignment of magnetic axes can be simulated by allowing λ to vary from either of its limits with rising temperature. It is in favor of our model that moderate departures from either extreme value of λ involve changes in sign of anisotropy coefficients, for this is consistent with the fact that the values of these coefficients fall to very low values long before the Curie point is reached. The quantitative agreement could be bettered in most cases by adjusting the relative radius, ρ, of the sphere on which the dicircles are supposed to lie. It seemed better to carry out the analysis without such refinements. The next logical step would seem to be the inclusion of strain effects, hitherto only considered for dipole magnets at atom centers.

It is a pleasure to acknowledge the part taken

in this development of ferromagnetic theory by Dr. R. M. Bozorth of the Bell Telephone Laboratories, whose acute suggestion of the difference in shape between elementary magnets in nickel and in iron[9] was the starting point of my renewed interest in computing magnetic interactions in ferromagnetic crystals, and with whom I have discussed ferromagnetic anisotropy on many occasions, both before and after undertaking the present analysis.

Appendix I

Convergent series for zonal harmonic lattice sums

The notation here used is especially convenient for numerical computations.

Taking a lattice point as origin, let the vector distance to any other point be $\mathbf{R}=ar\mathbf{r}$ where a is the length of a convenient edge of the unit cell, r is a numerical multiplier, and $\mathbf{r}$ is a unit vector in the proper direction. In the cubic system a is an edge of the unit cube, in the hexagonal system a is an edge of the rhombus forming the base of the unit prism. Let r_1, r_2, r_3 be numerical factors expressing the coordinates of any point in terms of the three edges of the unit cell, a corresponding to r_1. In the cubic system,

$$r^2=r_1^2+r_2^2+r_3^2; \quad \text{and} \quad \overline{r_i^2r_j^2}=(r_2^2r_3^2+r_3^2r_1^2+r_1^2r_2^2)/3.$$

In the hexagonal system,

$$r^2=r_1^2-r_1r_2+r_2^2+r_3^2c^2,$$

where c is the axial ratio, the ratio of the prism height to a. For abbreviation put

$$r_{12}^2=r_1^2-r_1r_2+r_2^2, \quad \text{and} \quad l_{12}^6=r_1^2r_2^2(r_1-r_2)^2.$$

Let n_r be the number of points obtained by permuting $\pm r_1$, $\pm r_2$, $\pm r_3$ in ways consistent with the symmetry of the lattice. (In the hexagonal system, for example, $\pm r_3$ does not permute with $\pm r_1$ and $\pm r_2$.)

Let a lattice reciprocal to the $\mathbf{R}$ lattice be defined by its vectors $\mathbf{Q}=a^{-1}q\mathbf{q}$, and by the equations

$$(\mathbf{q}_i\mathbf{r}_j)=\begin{cases}0 & i\neq j.\\ 1 & i=j\end{cases}$$

Here again q is a numerical multiplier, and $\mathbf{q}$ a unit vector. Let q_1, q_2, q_3 be numerical factors expressing the coordinates of any point in terms of the three edges of the unit cell (but a^{-1} is not in general the edge parallel to $\mathbf{q}_1$). In the cubic system,

$$q^2=q_1^2+q_2^2+q_3^2; \quad \text{and} \quad q_i^2q_j^2=(q_2^2q_3^2+q_3^2q_1^2+q_1^2q_2^2)/3.$$

In the hexagonal system

$$q^2=(4/3)(q_1^2+q_1q_2+q_2^2)+q_3^2c^{-2}.$$

For abbreviation put

$$q_{12}^2=(4/3)(q_1^2+q_1q_2+q_2^2),$$

and

$$k_{12}^6=(64/27)q_1^2q_2^2(q_1+q_2)^2.$$

The selection rules for r_1, r_2, r_3 and for q_1, q_2, q_3 may be stated as follows.

In primitive lattices $r_1, r_2, r_3, q_1, q_2, q_3$ must be integers and f, a factor in q terms for the hexagonal system, is unity. In body-centered lattices, $2r_1, 2r_2, 2r_3$, (r_2+r_3), (r_3+r_1), (r_1+r_2), q_1, q_2, q_3, $(q_1+q_2+q_3)/2$ must be integers. In face-centered lattices, $2r_1, 2r_2, 2r_3$, $(r_1+r_2+r_3)$, q_1, q_2, q_3, $(q_2+q_3)/2$, $(q_3+q_1)/2$, $(q_1+q_2)/2$ must be integers. In hexagonal close-packing q_1, q_2, q_3, and *either* r_1, r_2, r_3 *or* $(r_1-2/3)$, $(r_2-1/3)$, $(r_3-1/2)$ must be integers; if $(4q_1+2q_2+3q_3)/6$ is an integer, $f=2$; if $(4q_1+2q_2+3q_3\pm1)/6$ is an integer, $f=3/2$; if $(4q_1+2q_2+3q_3\pm2)/6$ is an integer, $f=1/2$; and if $(4q_1+2q_2+3q_3\pm3)/6$ is an integer, $f=0$. In all the summations the origin of coordinates, $r_1=r_2=r_3=0$, or $q_1=q_2=q_3=0$, is to be omitted.

A numerical parameter ϵ, which appears in each term of the formulae, may be given any convenient value provided it is the same in all terms. The product $\epsilon r=x$ appears as the argument of a series of numerical factors depending upon the probability integral. These are defined by the equations

$$\begin{aligned}
g_0(x)&=x^{-1}\Big[1-\frac{2}{\pi^{\frac{1}{2}}}\int_0^x e^{-\alpha^2}d\alpha\Big],\\
g_1(x)&=x^{-2}[g_0(x)+(2/\pi^{\frac{1}{2}})e^{-x^2}],\\
g_2(x)&=x^{-2}[3g_1(x)+(4/\pi^{\frac{1}{2}})e^{-x^2}],\\
g_3(x)&=x^{-2}[5g_2(x)+(8/\pi^{\frac{1}{2}})e^{-x^2}],\\
g_4(x)&=x^{-2}[7g_3(x)+(16/\pi^{\frac{1}{2}})e^{-x^2}],\\
g_5(x)&=x^{-2}[9g_4(x)+(32/\pi^{\frac{1}{2}})e^{-x^2}],\\
g_6(x)&=x^{-2}[11g_5(x)+(64/\pi^{\frac{1}{2}})e^{-x^2}].
\end{aligned} \tag{23}$$

Second-order sums

Cubic:—

$$S_2=(\epsilon^3/6)Sn_rx^2g_2(x)-(\epsilon^3/2)Sn_rg_1(x) -(2\pi/3)Sn_q\exp(-\pi^2q^2/\epsilon^2)+2\epsilon^3/3\pi^{\frac{1}{2}}. \tag{24}$$

Hexagonal:—

$$S_{20}=(\epsilon^3/4)Sn_rr_{12}^2r^{-2}x^2g_2(x)-(\epsilon^3/2)Sn_rg_1(x) -(2\pi\sqrt{3}/3c)Sfn_qq_{12}^2q^{-2}\exp(-\pi^2q^2/\epsilon^2)+2\epsilon^3/3\pi^{\frac{1}{2}}, \tag{25}$$

$$S_{22}=-(\epsilon^3/4)Sn_r(r_{12}^2-2r_3^2c^2)r^{-2}x^2g_2(x) +(2\pi\sqrt{3}/3c)Sfn_q(q_{12}^2-2q_3^2c^{-2})q^{-2}\exp(-\pi^2q^2/\epsilon^2). \tag{26}$$

Fourth-order sums

Cubic:—

$$S_{40}=(\epsilon^5/72)Sn_r(1-6\overline{r_i^2r_j^2}r^{-4})x^4g_4(x)-(\epsilon^5/12)Sn_rx^2g_2(x) +(\epsilon^5/8)Sn_rg_2(x)+(2\pi^3/9)Sn_q(q^4-6\overline{q_i^2q_j^2})q^{-2} \times\exp(-\pi^2q^2/\epsilon^2)-\epsilon^5/5\pi^{\frac{1}{2}}, \tag{27}$$

$$S_{40}=(\epsilon^5/180)Sn_r(1-15\overline{r_i^2r_j^2}r^{-4})x^4g_4(x)+(4\pi^3/45)Sn_q(q^4-15\overline{q_i^2q_j^2})q^{-2}\exp(-\pi^2q^2/\epsilon^2). \quad (27a)$$

Hexagonal:—

$$S_{40}=(\epsilon^5/64)Sn_r r_{12}^4r^{-4}x^4g_4(x)-(\epsilon^5/8)Sn_r r_{12}^2r^{-2}x^2g_3(x)+(\epsilon^5/8)Sn_r g_2(x)+(\pi^3\sqrt{3}/6c)Sfn_q q_{12}^4q^{-2}\times\exp(-\pi^2q^2/\epsilon^2)-\epsilon^5/5\pi^4, \quad (28)$$

$$S_{40}=(\epsilon^5/320)Sn_r(r_{12}^4-4r_{12}^2r_3^2c^2)r^{-4}x^4g_4(x)-(\epsilon^5/80)Sn_r(r_{12}^2-2r_3^2c^2)r^{-2}x^2g_3(x)+(\pi^3\sqrt{3}/30c)Sfn_q(q_{12}^4-4q_{12}^2q_3^2c^{-2})q^{-2}\times\exp(-\pi^2q^2/\epsilon^2), \quad (28a)$$

$$S_{40}=(\epsilon^5/2240)Sn_r(3r_{12}^4-24r_{12}^2r_3^2c^2+8r_3^4c^4)r^{-4}x^4g_4(x)+(\pi^3\sqrt{3}/210c)Sfn_q(3q_{12}^4-24q_{12}^2q_3^2c^{-2}+8q_3^4c^{-4})q^{-2}\exp(-\pi^2q^2/\epsilon^2). \quad (28b)$$

There are some errors in formulae corresponding to (28), (28a), (28b), in Phys. Rev. **44**, 38–42 (1933). In particular Eqs. (37), (38), (42), (43), (44), (46) of that paper are incorrect. Numerical results were correctly reported, nevertheless.

Sixth-order sums

Cubic:—

$$S_{60}=(\epsilon^7/2160)Sn_r(1-9\overline{r_i^2r_j^2}r^{-4}+3r_1^2r_2^2r_3^2r^{-6})x^6g_6(x)-(\epsilon^7/144)Sn_r(1-6\overline{r_i^2r_j^2}r^{-4})x^4g_5(x)+(\epsilon^7/48)Sn_rx^2g_4(x)-(\epsilon^7/48)Sn_rg_3(x)-(4\pi^5/135)Sn_q(q^6-9\overline{q_i^2q_j^2}q^2+3q_1^2q_2^2q_3^2)q^{-2}\times\exp(-\pi^2q^2/\epsilon^2)+\epsilon^7/21\pi^4. \quad (29)$$

$$S_{60}=(\epsilon^7/14400)Sn_r(2-33\overline{r_i^2r_j^2}r^{-4}+21r_1^2r_2^2r_3^2r^{-6})x^6g_6(x)-(\epsilon^7/720)Sn_r(1-15\overline{r_i^2r_j^2}r^{-4})x^4g_5(x)-(\pi^5/225)Sn_q(2q^6-33\overline{q_i^2q_j^2}q^2+21q_1^2q_2^2q_3^2)q^{-2}\times\exp(-\pi^2q^2/\epsilon^2), \quad (29a)$$

$$S_{60}=(\epsilon^7/16800)Sn_r(2-63\overline{r_i^2r_j^2}r^{-4}+231r_1^2r_2^2r_3^2r^{-6})x^6g_6(x)-(2\pi^5/525)Sn_q(2q^6-63\overline{q_i^2q_j^2}q^2+231q_1^2q_2^2q_3^2)q^{-2}\times\exp(-\pi^2q^2/\epsilon^2). \quad (29b)$$

Hexagonal:—

$$S_{63}=-(\epsilon^7/720)Sn_r r_{12}^6r^{-6}x^6g_6(x)+(\epsilon^7/40)Sn_r r_{12}^4r^{-4}x^4g_5(x)-(\epsilon^7/10)Sn_r r_{12}^2r^{-2}x^2g_4(x)+(\epsilon^7/15)Sn_r g_3(x)+(8\pi^5\sqrt{3}/135c)Sfn_q q_{12}^6q^{-2}\exp(-\pi^2q^2/\epsilon^2)-16\epsilon^7/105\pi^4. \quad (30)$$

$$S_{63}=-(\epsilon^7/5040)Sn_r(r_{12}^6-6r_{12}^4r_3^2c^2)r^{-6}x^6g_6(x)+(\epsilon^7/420)Sn_r(r_{12}^4-4r_{12}^2r_3^2c^2)r^{-4}x^4g_5(x)-(\epsilon^7/210)Sn_r(r_{12}^2-2r_3^2c^2)r^{-2}x^2g_4(x)+(8\pi^5\sqrt{3}/945c)Sfn_q(q_{12}^6-6q_{12}^4q_3^2c^{-2})q^{-4}\times\exp(-\pi^2q^2/\epsilon^2). \quad (30a)$$

$$S_{63}=-(\epsilon^7/15120)Sn_r(r_{12}^6-12r_{12}^4r_3^2c^2+8r_{12}^2r_3^4c^4)r^{-6}x^6g_6(x)+(\epsilon^7/7560)Sn_r(3r_{12}^4-24r_{12}^2r_3^2c^2+8r_3^4c^4)r^{-4}x^4g_5(x)+(8\pi^5\sqrt{3}/2835c)Sfn_q(q_{12}^6-12q_{12}^4q_3^2c^{-2}+8q_{12}^2q_3^4c^{-4})q^{-2}\exp(-\pi^2q^2/\epsilon^2). \quad (30b)$$

$$S_{63}=-(\epsilon^7/166320)Sn_r(5r_{12}^6-90r_{12}^4r_3^2c^2+120r_{12}^2r_3^4c^4-16r_3^6c^6)r^{-6}x^6g_6(x)+(8\pi^5\sqrt{3}/31185c)Sfn_q(5q_{12}^6-90q_{12}^4q_3^2c^{-2}+120q_{12}^2q_3^4c^{-4}-16q_3^6c^{-6})q^{-2}\exp(-\pi^2q^2/\epsilon^2). \quad (30c)$$

$$S_{66}=(\epsilon^7/46080)Sn_r(2r_{12}^6-27l_{12}^6)r^{-6}x^6g_6(x)+(\pi^5\sqrt{3}/1080c)Sfn_q(2q_{12}^6-27k_{12}^6)q^{-2}\times\exp(-\pi^2q^2/\epsilon^2). \quad (31)$$

Erratum: The Sign of the Magnetic Moment of the K^{39} Nucleus

H. C. TORREY
Columbia University, New York City

(Phys. Rev. **51**, 501 (1937))

THE title of Fig. 6, p. 506 should read as follows:

"Fig. 6. Asymmetries in deflection patterns of (a) $m=-1$ atoms with negative strong field moments, (b) $m=-1$ atoms with positive strong field moments."

The description of these curves in the text is correct.

The Ionization of Neon, Krypton and Xenon by Bombardment with Accelerated Neutral Argon Atoms*

HAROLD WAYLAND†
California Institute of Technology, Pasadena, California
(Received April 8, 1937)

A series of experiments on the ionization of noble gases by accelerated noble gas atoms, with an electrometer method, is described. Preliminary measurements by Beeck showing little velocity dependence for ionization of argon by argon atoms between 50 and 100 volts, and showing an ionization of neon by argon atoms in this energy range are shown to be due mostly to secondary effects—principally to argon radiation. Positive evidence is given for the ionization of one noble gas by atoms of another, and onset potentials for ionization are found to be: 55 volts for argon bombarding xenon; 50 volts for argon bombarding krypton, and approximately 130 volts for argon bombarding neon.

CERTAIN of the onset potentials for the ionization of noble gases by neutral noble gas atoms have been measured recently by Varney.[1] By using a balanced space-charge method devised by Lawrence and Edlefsen,[2] and improved by Varney,[3] he was able to measure the onset potentials for ionization of Ne by Ne, A by A, Kr by Kr, and Xe by Xe. Later work with a space-charge detector in conjunction with an apparatus designed to permit different gases to be used for target and projectile gave no measurable results for A in Kr or Xe.[4] The author, after a similar failure with the balanced space-charge method, then undertook to make such measurements using an electrometer method, similar to that employed by Beeck[5] for studying the ionization of noble gases by positive ion bombardment. The space-charge detector possesses many advantages over an electrometer method, since it measures only positive ions, while the latter also measures secondary electrons, which tend to obscure the real effect. Secondaries were found to play a very important role, but it is believed that the evidence for the ionization of Ne, Kr, and Xe by neutral A atoms is definite.

APPARATUS

A diagram of the apparatus is shown in Fig. 1. It is similar in construction to that used by Beeck[6] and the author,[7] except no velocity filter was used, in order to maintain the intensity of the neutral beam for low energies. Positive ions of the gas used as a projectile were formed in chamber I by electron bombardment from a hot tungsten filament. A mixture of ions and unionized gas diffused through slit 1 (slits 1, 2, 3, and 4 were 0.5 mm wide and 5 mm long; slit 1 was 8 mm deep, and the others 5 mm deep). The ions were picked up by an electrostatic field between slits 1 and 2. The ion beam reaching chamber III should be quite homogeneous, since the ions would diffuse from slit 1 with only gas kinetic velocities. The pressure in chamber II was kept low enough (chambers II and IV were evacuated by high speed mercury diffusion pumps) so that there would be few neutralizing collisions between slits 1 and 2. Chamber III was filled with the same gas as chamber I, so that part of the ion beam would be neutralized by charge transfer, a method first employed for this type of work by Beeck.[8] From slit 3 there emerged a mixed beam of ions and neutrals, from which the positives were removed by applying a retarding potential to slit 4. Secondary electrons were deflected out of the beam by the field of a small permanent magnet *m*. The

* Part of a thesis presented in partial fulfillment of the requirements for the degree of Doctor of Philosophy at the California Institute of Technology.

† At present Fellow of the American-Scandinavian Foundation in Copenhagen, Denmark.

[1] R. N. Varney, Phys. Rev. **50**, 159 (1936).

[2] E. O. Lawrence and N. E. Edlefsen, Phys. Rev. **34**, 284 (1929).

[3] R. N. Varney, Phys. Rev. **47**, 483 (1935).

[4] R. N. Varney. Private communication.

[5] O. Beeck, Ann. d. Physik **6**, 1001 (1930).

[6] O. Beeck, Ann. d. Physik **19**, 121 (1934).

[7] O. Beeck and H. Wayland, Ann. d. Physik **19**, 129 (1934).

[8] O. Beeck, Proc. Nat. Acad. Sci. **18**, 311 (1932).

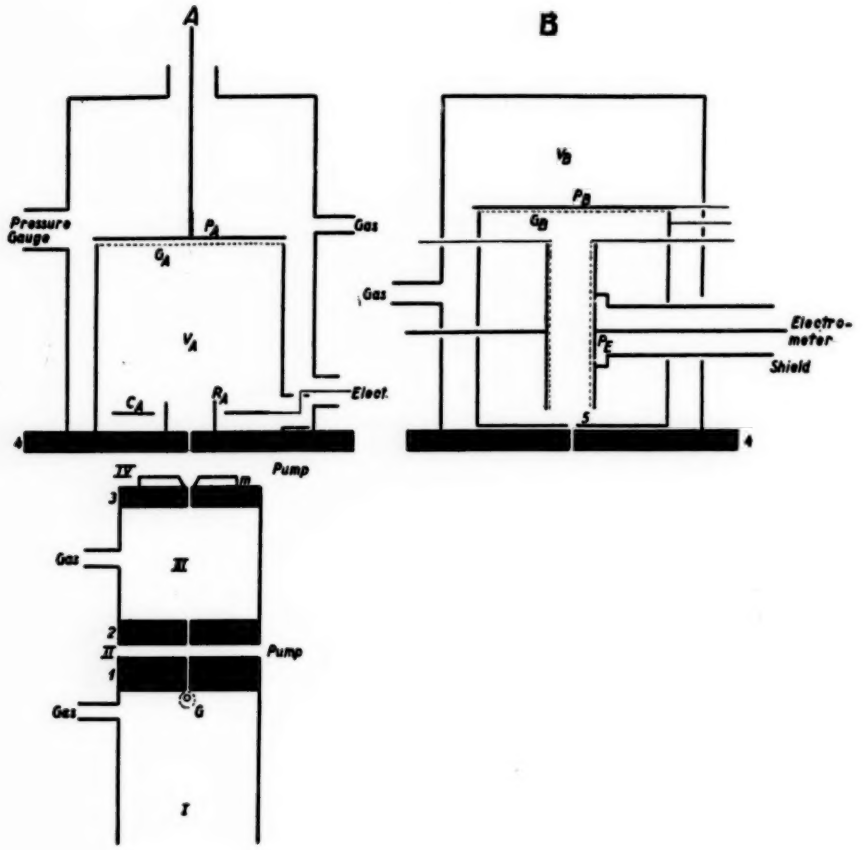

FIG. 1. Diagram of the apparatus.

resulting neutral beam then entered chamber V where its effects on various gases could be measured.

Two different measuring chambers were used for the study of the ionization. The first, V_A Fig. 1, proved to be useful only in determining the origin of the most important secondary effects. This arrangement was a modification of that used by Sutton and Mouzon,[9] and by Beeck[5] in their work on the ionization of gases by positive ion bombardment. A collecting ring C_A, protected by a guard ring R_A from impacts by the atom beam, was made positive with respect to the grid G_A. This field brought any electrons formed in the chamber—both primary and secondary—to the collector.

The actual onset potential measurements were made with arrangement V_B. In this apparatus, a parallel plate guard-ring condenser was used for collecting the electrons, giving a much more uniform collecting field. In addition, the major metal surfaces were protected by grids, which could be adjusted to such potentials as largely to suppress the secondary electron emission. The grids protecting the condenser plates were made of 2-mil Ni wire soldered to narrow brass frames. The wires were mounted 1 mm apart, and the front of the grid was 1 mm from the plate it covered. P_E was the actual collecting plate. The electrometer lead was electrostatically shielded by a brass tube, which also formed the support for the guard ring. The measuring chamber was insulated from the vacuum chamber by a ring of Bakelite BT 61, so that slits 4 and 5 were 1 mm apart. This allowed slit 5 to be made negative with respect to slit 4 in order to hold back secondary electrons formed in slit 4.

All surfaces except the grids and their frames were blackened with benzol soot to cut down

[9] R. M. Sutton and J. C. Mouzon, Phys. Rev. **35**, 694 (1930).

secondary emission, and to avoid reflection of radiation. The grids and grid frames were blackened with Aquadag—colloidal graphite in aqueous solution—since the heat of the sooting flame was sufficient to warp the grids.

The electrometer used for the measurements of the electron current was a Wulff string electrometer with a maximum usable sensitivity of 1000 scale divisions per volt, although it was usually employed at about half this sensitivity.

The gases were admitted to the various chambers through Smythe[10] leaks from 300 cc gasometer bulbs for A and Ne, and 100 cc bulbs for Kr and Xe. The A and Ne were obtained in pure form in liter flasks from the Air Reduction Sales Company. The Kr and Xe were left over from bulbs given to Beeck by the Linde A.G. in Germany. Since these gases had been sealed in only by stopcocks for several years, their purity was checked spectroscopically. The only contamination found was Hg vapor, which the trapping system failed to remove completely from the discharge tube. The A and Ne were passed through a liquid-air trap, and Kr and Xe through a CO_2 trap before being admitted to the apparatus.

The pressures used in chambers I and III were measured by vibration gauges. The readings of the gauges which corresponded to maximum emission were obtained empirically and used in adjusting the leaks, without attempting to measure the absolute values of the pressures. In the measuring chamber the pressure was measured on a McLeod gauge connected to the chamber through a trap cooled with liquid air for A and Ne, and with solid CO_2 and alcohol for Kr and Xe.

When the gas in the top chamber differed from that used for producing the atom beam, it was impossible to use a sufficiently high pressure in the neutralizing chamber to insure the maximum efficiency of neutralization, since interdiffusion would contaminate the gas being bombarded. Consequently the pressure in the neutralization chamber was adjusted to such a value that the pressure in the upper chamber was at most 2×10^{-4} mm of Hg, when no gas was admitted directly to that chamber. Since the lowest pressure used in the upper chamber was 2×10^{-3} mm of Hg, the contamination was kept to 10 percent or less.

[10] W. R. Smythe, Rev. Sci. Inst. **7**, 435 (1936).

Measurements

Collecting arrangement A.

In this arrangement, only the surface which was struck by the direct atom beam was protected by a grid. Consequently any secondary electrons knocked off the side walls by scattered atoms or radiation would be captured by the collector. For A in A, a very copious emission of electrons existed even for atom beams with energies below the value found by Varney for the onset. This emission also proved to be practically independent of the presence or absence of positive ions in the beam. Brasefield[11] interpreted similar results as indicative of an exceedingly high coefficient of emission of secondary electrons from metal surfaces when bombarded by neutral atoms. Rostagni's measurements,[12] however, showed that Brasefield's value was much too high. Photoelectric effect was believed to be responsible for the difference.

In the present work, the radiation from the filament did not knock off enough photoelectrons to be measurable at the sensitivity used, which allowed a current of about 1×10^{-14} amperes to be measured. However, as soon as the electrons from the filament were accelerated with sufficient energy to ionize, and consequently to excite, the A in the lower chamber, the effect began to show up. A beam consisting only of 60 volt A positives and radiation—chamber III was evacuated—was allowed to bombard the upper chamber. With no gas admitted to V_A, a potential of 20 volts applied to P_A reduced the current to the collector to 16 percent of its value when P_A and G_A were at the same potential. With A at a pressure of 8×10^{-3} mm in V_A, and the same bombarding beam, 20 volts applied to P_A reduced the current collected only to 73 percent of its original value. With Ne in V_A at a pressure of 1.5×10^{-2} mm, a potential of 20 volts on the plate reduced the current collected to 34 percent of its original value. The large amount of ionization apparently coming from the body of the gas in the A-A case

[11] C. J. Brasefield, Phys. Rev. **44**, 1002 (1933).

[12] A. Rostagni, Zeits. f. Physik **88**, 55 (1934) and Nuovo Cimento **11**, 99 (1934).

could not possibly have been due to ionization. Even for a bombarding beam of neutrals, the ionization at 60 volts had been found to be only a small fraction of the background, and in this case the neutral component must have been very small. The positives could have caused no ionization, as the onset for ionization of A by A^+ is about 300 electron volts.[13] * Cutting off the ion beam by a retarding potential made only a small difference, so the principal effect must have been due to scattering of the A radiation formed in the discharge. The A radiation is absorbed by the A in V_A, and reemitted in all directions, knocking secondary electrons off the side walls. Ne would show no such selective effect for A radiation, and consequently would not show so strong an effect, just as observed.

This copious emission of secondaries by the radiation gives experimental evidence for the discrepancy between his and Brasefield's results. It also accounts for the copious "ionization" of both A and Ne by A neutrals with *little velocity dependence* of the intensity of ionization between 50 and 100 volts found by Beeck[8] with an apparatus almost completely unprotected from photoemission. The fact that for A in A he found almost as many positives as negatives is readily explained. If the collecting field is such as to remove the photoelectrons from the plate connected to the electrometer, the string will be charged up positively. Consequently, the only difference between "positives" and negatives will be due to secondary electrons formed elsewhere, and to the small amount of ionization present. In the case of Ne, he would naturally observe fewer positives because the Ne is not so efficient in scattering the A radiation, and the relative importance of secondaries from other parts of the apparatus to those from the condenser plates is much greater.

Collecting Head B

In this apparatus the secondary emission could be suppressed by making the grids covering the major surfaces negative with respect to those surfaces. The effect of varying the collecting potential between the condenser plates, and that of varying the potentials of the grids with respect to the plates are shown in Fig. 2. It is seen from the coincidence of the 6 and 12 volt curves that grid potentials above 6 volts are sufficient to give a minimum of secondaries. Fig. 2 also shows that a collecting potential of 30 volts gives virtual saturation, while one of only 12 volts is sufficient for 90 percent of saturation.

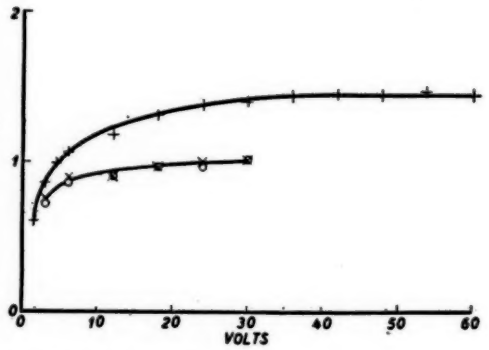

Fig. 2. Collecting potential required for saturation. Abscissae: collecting potential on condenser in volts. Ordinates: electron current to arbitrary scale. Legend: + grids at 0 volts; ○ grids at −6 volts; × grids at −12 volts.

The secondary electrons emitted from P_B could be held to a minimum by making it $22\frac{1}{2}$ volts positive with respect to G_B. Below G_B an attempt was made to keep the various potential differences low enough that electrons accelerated by them would not have sufficient energy to ionize the gas in the chamber, although actual measurements showed that the position of an inset was not affected by varying the collecting potential or the grid potentials. Slit 5 was made negative with respect to slit 4, 45 volts giving a minimum of secondaries.

In spite of all these precautions, secondary electrons formed a fair percentage of the total effect measured, but it was possible to get effects which seem attributable only to ionization of the gas by atom collision. Actual measurements were made collecting negatives, but in all cases except Ne in Ne a check run was made collecting positives to be sure that they were present. Since a collecting potential of 60 volts was required even to approach saturation for positives, it was deemed advisable not to attempt to collect them for an actual determination of the

[13] F. Wolf, Zeits. f. Physik **74**, 575 (1932).

* *Note added in proof:* Recent work by F. Wolf (Ann. d. Physik **29**, 33 (1937)) indicates that the onset of ionization of A by A^+ may occur below 100 volts. The efficiency indicated in his experiments is so low as not to affect the validity of the arguments presented here.

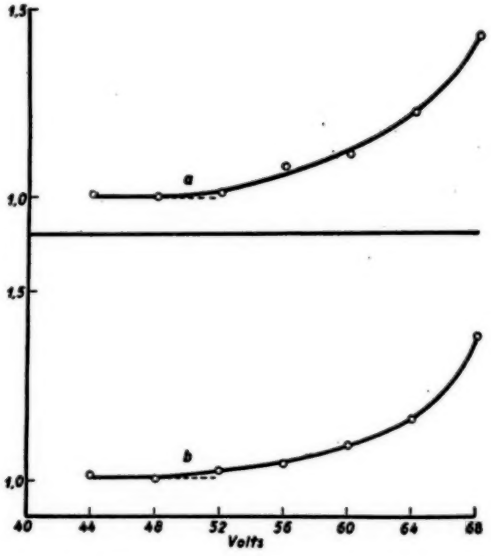

FIG. 3. Ionization of A by A neutrals. Abscissae: atom accelerating potential in volts. Ordinates: ionization current collected, reduced to background as unity.

onset, since both primary and secondary electrons would have enough energy to ionize the gas. Using low enough collecting potentials to be sure of no ionization by the electrons gave such small currents that no good determination of the onset could be made.

Runs were made as quickly as possible to avoid pressure changes, and warping of the filament as the supports became heated. The data taken under different conditions could not be reduced to a common basis by any method of correction that presented itself, so data were plotted run for run, and the onset potential obtained from comparing various runs. A point below the onset was taken as a standard, and a measurement of the current to the collecting plate was taken for this accelerating potential. The accelerating potential was then changed, and the current measured again. The acceleration was then returned to the standard value, and if the current collected had not changed appreciably, the run was continued. If the current collected at the standard points drifted slowly downward, as would be expected from decreasing pressures, the run was used. If, however, the standard was erratic, or drifted very rapidly, so that interpolation was dangerous, the run was thrown out. Data were generally plotted in relation to the background as unity, as this gives a good idea of the reliability, and absolute values are unnecessary for the location of the onset potentials.

ARGON IN ARGON

A in A gave not only the largest ionization currents of any of the combinations tried, but it also gave the largest absolute value of the background. Many runs were taken with A in A in learning to manipulate the apparatus, but very few data were taken under the conditions required for a "usable" run. The practice runs gave an indication that ionization set in in the neighborhood of 50 volts. The two runs which fulfilled the required conditions for steadiness are given in Fig. 3. It will be seen that the check with Varney's value of 48 volts ± 2 volts is excellent—so good that no further work with A in A was deemed necessary.

NEON IN NEON

The efficiency of ionization of Ne by Ne is very small, and in addition it is very difficult to get an intense neutral beam. In the only curve obtained for this case, Fig. 4, it is seen that the rise above

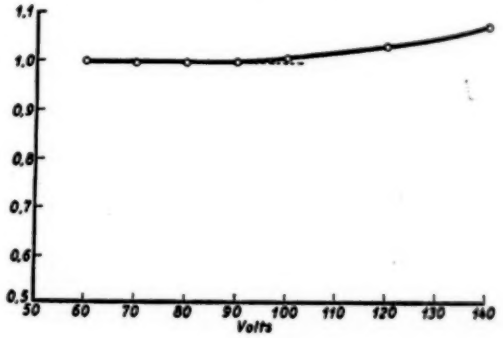

FIG. 4. Ionization of Ne by Ne neutrals. Abscissae: atom accelerating potentials in volts. Ordinates: ionization current collected, reduced to background as unity.

the background is small. The likelihood of obtaining a measurement for the onset which could be compared in precision with Varney's was deemed to be so small that further work with Ne as a bombarding agent was abandoned.

ARGON IN NEON

From a beam of A neutrals, with Ne in the ionizing chamber, curves *b*, *c*, *d*, and *e*, Fig. 5, were obtained. Curves *b*, *c*, and *d* gave promise

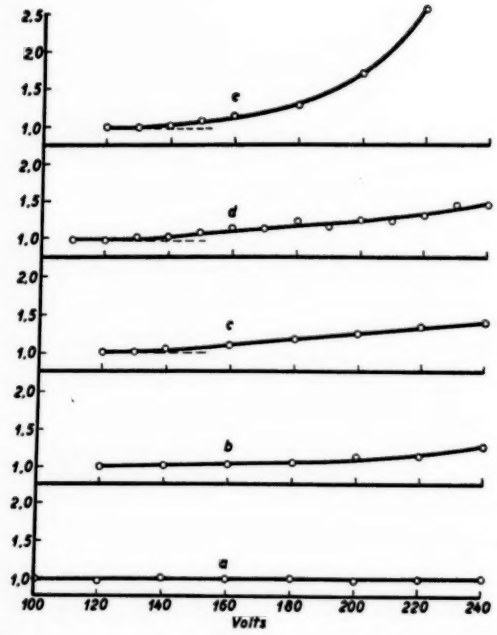

FIG. 5. Ionization of Ne by A neutrals. Abscissae: atom accelerating potentials in volts. Ordinates: ionization current collected, reduced to background as unity. Collecting potential 30 volts; grids 12 volts. Neon pressures: 4.5×10^{-3} mm Hg for *b*, 9.5×10^{-3} for *c*, 4.5×10^{-3} for *d*, and 1.6×10^{-2} for *e*.

that Ne really was ionized by A neutrals, and curve *e*, taken at a considerably higher pressure, gives definite evidence of ionization, and indicates the region of onset. Preliminary experiments showed no measurable rise in the curve below 120 volts. In order to ascertain the effect due to the residual A in the upper chamber, a run was taken over this energy range with the Ne shut off. This is shown in Fig. 5*a*, the flatness of which indicates that the effect in Ne is real, with ionization occurring above 130 volts.

ARGON IN XENON

Fig. 6 shows the results obtained for A bombarding Xe. Curves *a* and *b* gave the region of onset, using Xe pressures of about 4×10^{-3} mm of Hg. For the other measurements, the McLeod was out of order, so the pressure was not known accurately, but was estimated from a vibration gauge to be higher than for the first run. Two runs were attempted, the data for the first being given in curve *c*. The warping of the filament, with a resulting drop in the intensity of the atom beam, prevented the successful completion of the second run. Both runs, however, gave evidence of a definite break in the curve between 55 and 60 volts, as shown so clearly in curve *c*. Sufficient gas was not at hand to make further runs.

ARGON IN KRYPTON

The results for A in Kr are shown in Fig. 7. Curves *a* and *b* were taken quickly to establish the general region of onset, using low pressures to conserve gas. The pressure was then raised and curve *c* taken at 5 volt intervals. The flatness of the curve below 50 volts indicated that the onset must occur at that point or above, so curve *d* was taken with 2 volt intervals. The pressure was beginning to fall rapidly, so no further curves were taken. Although the major differences in background are due to the different pressures used, the intensity of the A beam may very well have dropped during the sequence of runs. Immediately after the last run, all of the gas was turned off, and the system allowed to pump down to a pressure of about 10^{-5} mm. Then the stopcocks leading from the leaks to chambers I and III were reopened, and the system allowed to come to equilibrium. The A pressure in the upper chamber was found to be 2×10^{-4} mm. The filament was then turned on, and a background set of readings was taken, Fig. 7*e*. It is apparent

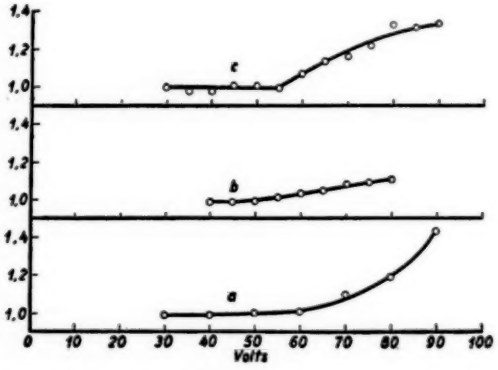

FIG. 6. Ionization of Xe by A neutrals. Abscissae: atom accelerating potentials in volts. Ordinates: ionization current collected, reduced to background as unity. Collecting potential 30 volts; grid potentials 12 volts.

from this that the onset for ionization of Kr by A in the neighborhood of 50 volts is real. The shape of the background curve also leaves little doubt as to the reality of the effect in xenon.

Discussion of Results

The conclusions to be drawn from the work with chamber V_A have already been discussed. Chamber V_B afforded the possibility of measuring the onset potentials for ionization of A, Ne, Kr, and Xe by A neutrals. The check with Varney's value for A in A makes this work directly romparable with his in studying the variation of onset potential with change of target atom. His cesults are given in parentheses in Table I, while those of this work are given without parentheses. It is interesting to note that the onset potential rises as we progress from the diagonal, as predicted by the simple theory of Zwicky.[14] The actual value for the onset in the case of A in Ne cannot be taken too seriously, as the rise of the curve is so slow. The value for A in Xe is considerably better, although it is true that curve *b* suggests that there may be some effect below the 55 volts assigned to the onset. This may have been due to the A background, as the total rise is not great in this case. The case for A in Kr is certainly the most clean cut. Here there can be no question that a marked effect sets in just above 50 volts.

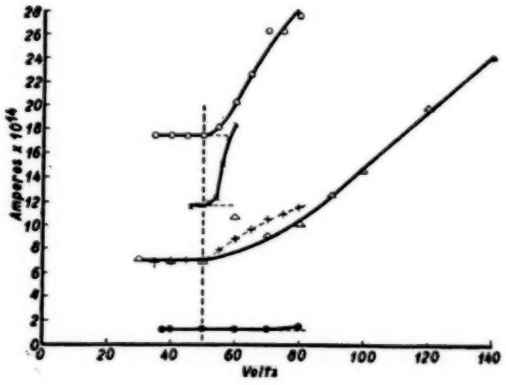

Fig. 7. Ionization of Kr by A neutrals. Abscissae: atom accelerating potential in volts. Ordinates: ionization current collected, in amperes $\times 10^{14}$. Legend: △ curve *a*; + curve *b*; ○ curve *c*; × curve *d*; ⊕ curve *e*. Collecting potential 30 volts; grids 12 volts. Krypton pressures: 3.3×10^{-3} mm Hg for *a* and *b*; 9×10^{-3} for *c*, and 7×10^{-3} for *d*.

[14] F. Zwicky, Proc. Nat. Acad. Sci. **18**, 313 (1932).

Table I. *Ionization potentials (in electron volts) for ionization of gases by bombardment with noble gas atoms. Varney's results in parentheses.*

Bombarding Atoms	Target Atoms			
	Ne	A	Kr	Xe
Ne	(74)			
A	130?	48 (48)	50	55
Kr			(40)	
Xe				(35)

All of the curves, with the possible exception of those for A in Kr, tend to indicate that the onset for ionization by atom bombardment is not sharp. For the A-Kr case, if we were to take curve *c*, Fig. 7, we would be tempted to extrapolate back to 52 volts as a sharp inset. However, when a 52-volt point was taken, curve *d*, it is seen to make the curve swing into the background instead of cutting it sharply. The probability of ionization must rise sharply between 50 and 55 volts, but there may still be some ionization even at much lower potentials.

The author wishes to thank Dr. R. N. Varney of New York University, and Dr. Otto Beeck of the Shell Development Company for helpful discussions; and the staff of the Norman Bridge Laboratory of Physics of the California Institute of Technology for their cooperation in carrying out this research.

LETTERS TO THE EDITOR

Prompt publication of brief reports of important discoveries in physics may be secured by addressing them to this department. Closing dates for this department are, for the first issue of the month, the eighteenth of the preceding month, for the second issue, the third of the month. Because of the late closing dates for the section no proof can be shown to authors. The Board of Editors does not hold itself responsible for the opinions expressed by the correspondents.

Communications should not in general exceed 600 words in length.

The Sign of the Magnetic Moment of the Neutron

Previous experiments[1-3] have shown that slow neutrons may perform adiabatic transitions in a rotating magnetic field when the angular velocity of the field is approximately the same as the Larmor precession frequency of the neutron $\mu_n h/H$ and are consistent with a value for the neutron moment μ_n of the order of several NM. Recent experiments by Frisch, von Halban and Kogh[4] confirm this.

The probability of a neutron making transitions in a precessing field has been calculated by Professor Rabi,[5, 6] and as he has suggested, both the sign and magnetic moment may be determined from the direction and magnitude of the precessing field.

An experiment has been performed using the arrangement in Fig. 1. Slow neutrons passing through the magnetized iron at A and B are partially polarized, as observed by the increase in neutron transmission for the magnetized as compared to the demagnetized case. A precessing field is set up in the region between the two magnets to cause reorientation of the neutron spins, and hence a decrease in the polarization effect. This field is produced by the superposition of a constant field parallel to the magnetization in the iron, and a rotating field due to two parallel wires, W_1 and W_2 carrying current in opposite directions. The appropriate expressions for the transition probability in this case where the neutrons are polarized in the direction of the constant field have been derived by Mr. Julian Schwinger:

$$P^{\frac{1}{2}}_{-\frac{1}{2}} = \frac{\mu_n^2 H_1^2}{\mu_n^2 H_1^2 + (\mu_n H_2 + (\hbar\omega/2))^2} \times \sin^2 (t/2\hbar)[\mu_n^2 H_1^2 + (\mu_n H_2 + (\hbar\omega/2))^2]^{\frac{1}{2}},$$

where μ_n is the neutron magnetic moment, H_1 the field due to the wires, H_2 the constant magnetic field, ω the angular velocity of the field, and t is the time the neutron spends in the field. The direction of the precessing field which gives the maximum reorientation determines the sign of the moment and the measured reorientation probability gives the value of the moment.

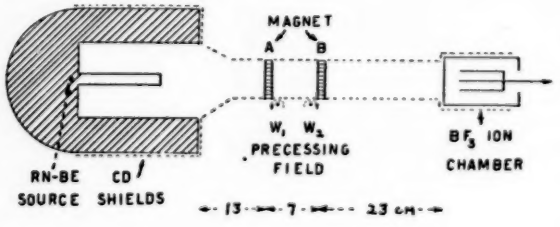

FIG. 1.

The special magnets at A and B were constructed by Dr. J. H Manley who kindly loaned them for this experiment. Slabs of Swedish iron 12 mm thick with Cd collimating strips interposed are magnetized to saturation by a small electromagnet. Stray fields are minimized.

TABLE I.

POLARIZING FIELD	ROTATING FIELD	NO./MIN.	* CHANGE IN %
Demag.	Zero	439.27±0.92	0±0.21
Mag. +	Zero	447.01±0.93	3.43±0.22
Mag. +	+	446.53±0.93	3.21±0.22
Mag. +	−	441.84±0.92	1.08±0.21
Fast neutron background with Cd		213.3	

* Slow neutron count only.

Conditions for complete reorientation of spins are practically impossible to obtain over such a large region. The arrangement used was based on calculations of Mr. Schwinger for complete reorientation in the center of the beam, assuming $\mu_n \sim 2$NM. The constant field parallel to the iron field is produced by controlling the stray field of the magnets through suitably placed iron pieces, and ranges from 8 to 14 gauss. Components of this field perpendicular to the iron field and the neutron direction have been shown to cause serious reorientation in this and other experiments and must be minimized. The wire field current was equivalent to 90 amperes for these conditions, with an effective rotation of the field of 180° at the center of the beam.

The results of a series of measurements are shown in Table I.

Without the precessing field, an increase of 3.43±0.22 percent is observed. With the precessing field in the + direction reorientation of the spins is small since the increase is still 3.21±0.22 percent. However, with the precessing field reversed, approximately 2/3 of the neutron spins are reoriented, reducing the effect to 1.08±0.21 percent.

The direction of the precessing field required to cause reorientation indicates that the neutron moment is negative. Because of the varying magnetic field values over such a large region, and the velocity distribution of the slow neutrons, accurate calculation of the magnitude of the moment is difficult. It is, however, consistent with the value of about −2NM as would be expected from the values of the proton and deuteron moments and could

hardly be smaller than -1, or larger than $-3NM$. Further refinements are in progress.

The suggestions of Professor Rabi and Mr. Schwinger have been very valuable.

P. N. POWERS
H. CARROLL
H. BEYER
J. R. DUNNING

Columbia University,
New York, N. Y.,
June 19, 1937.

[1] Dunning, Powers, Beyer, Phys. Rev. **51**, 51 (1937).
[2] Powers, Beyer, Dunning, Phys. Rev. **51**, 371 (1937).
[3] Powers, Carroll, Dunning, Phys. Rev. **51**, 1112 (1937).
[4] Frisch, von Halban, Kogh, Nature **139**, 756 (1937).
[5] Rabi, Phys. Rev. **51**, 683 (1937); **51**, 652 (1937).
[6] Schwinger, Phys. Rev. **51**, 648 (1937).

The Nuclear Exclusion Principle and the Neutron-Proton Pattern

This letter considers the neutron-proton pattern of the 305 atomic species now known in nature from the point of view of relations developed earlier.

1. Mass deviations from whole numbers of adjacent species are the best indications of nuclear stability, but when unknown the abundance gives an indication of stability (1915–17).

2. General stability relations: The stability is a function of the ratio of neutrons to protons (N/Z) and the atomic number Z. N/Z increases, as Z increases, from 1.00 to 1.6, but for more than 80 percent of all atoms $N=Z$. If N/Z is too large, negative electrons are emitted (1921).

3. Nuclei with even numbers of both protons and neutrons are much more abundant than those with either an odd neutron or proton, while nuclei in which both the number of neutrons (N) and of protons (Z) is odd are never stable unless $N=Z$ (1917–21), and then not if $Z>7$. On this basis all nuclei were divided into four classes (see Table I). For $N=Z$ Coulombic repulsion of protons gives the limits: Class I $Z \gtrsim 20$, Class IV $Z \gtrsim 7$.

From the composition of the meteorites it was assumed that the energy of binding (E) is about the same for classes II and III so $E_{ee}>E_{e0}>E_{00}$.

4. The number of isotopes with Z even is much larger, especially as the atoms become heavier, than with Z odd (1915).

5. The formula $(pn)_Z n_I$ represents the composition of all nuclei (1921).

The existence of deuterons, hydrogen nuclei of mass 3, and helium nuclei of mass 3, was assumed.

In speaking of the helium nucleus of mass 3, the writer in 1921 gave the following statement: "It is not unlikely that when the speed of such a particle is reduced it would either pick up a negative electron, and so be converted into an isotope of hydrogen, or it may pick up a neutron, giving an α-particle."[1]

6. The ratio N/Z is decreased by the emission of a β-particle but on account of the nuclear exclusion principle, stable isobars of class I differ in isotopic number (number of free neutrons) by 4, while isobars of classes II and III differ in isotopic number by 2. On account of the stability range in N/Z isobars of class I are numerous, of classes II and III, rare.

One isotope of the forbidden class (K^{40}) was predicted, but was assumed to be β-active (reference 1, p. 1050, diagram). This was discovered recently by Tate and Nier.

It remains to indicate in a few words how the above relations indicate just the neutron-proton pattern which is found. Shifts from one class to another occur by emission or capture of negative electrons, or by emission of positive electrons as follows: IV→I II↔III.

Atoms of class IV are never stable if an adjacent isobar of class I is stable. Thus H^2, Li^6, B^{10}, and N^{14} exist, and these alone, since for their isobars $I=\pm 2$, and -2 always represents instability. Also $+2$ gives values of N/Z which lie in the unstable region until O^{18} is reached. Since this atom of class I is stable, the adjacent isobar F^{18} is unstable, so N^{14} represents the upper limit for class IV.

7. Continuity and regularity of series: On any isotopic level all positrons in any series between Z minimum and maximum are filled. The 4 series involved are the n, $n+2$, or the two even series, and $n+1$, $n+3$, or odd series. The two even series by the exclusion principle never occupy the same level, unless $I=0$.

Odd series: Since the binding energy E_{e0} is about the same for both series, the two series become amalgamated to almost a single series in that they occupy the same levels, and have almost the same lower and upper limits for Z on any isotopic level. The stability range is so narrow in N/Z that in general an isotopic level begins and ends whenever two isotopes occur. Exceptions:

TABLE I. *Classification of nuclei.*

	Neutrons N	Protons Z	$N+Z=A$	Percentage of Material	
				Earth	Meteorites
Class I	Even	Even	Even	87.4	95.4
Class II	Even	Odd	Odd	10.8	2.1
Class III	Odd	Even	Odd	1.8	2.5
Class IV*a*	Odd	Odd	Even	0.000	0.000
b				0.007	0.0

Class IV*a* $N>Z$ Class IV*b* $N=Z$

1. If for example the $4n+3$ series, in a lower level, as with K^{39}, extends beyond the $4n+1$ series, leaving a blank (A^{37}) then there will also be a blank in the upper series for the isobar of the species (as A^{39}).

2. Isobars may exist, since E_{e0} is about the same for classes II and III, and should be expected most for not too small nor too large values of Z and A (stability condition). The known isobars of classes II and III are Rb and Sr 87, Ru and Rh 101, In and Sn 115, Sb and Te 123, and possibly Re and Os 187, and much less probably Hg and Th 203.

Shifts of level due to capture of neutrons, are often followed by β-changes, such as are discussed here.

WILLIAM D. HARKINS

Kent Chemical Laboratory,
University of Chicago,
Chicago, Illinois,
May 27, 1937.

[1] W. D. Harkins, J. Am. Chem. Soc. **43**, 1049 (1921).

Artificial Radioactivity Produced by Alpha-Particles

Continuing our survey[1,2] of radioactivity produced by an alpha-particle beam accelerated in a cyclotron, we have replaced the thin platinum window through which the alpha-particles emerged by a gate valve assembly. This change permits targets to be bombarded by the direct beam inside the cyclotron vacuum tank, and removed in about 30 seconds without impairing the vacuum in the tank proper. A four- to ten-fold enhancement of the activities we have already studied has resulted. The present beam has an energy of about 8 Mev, and the currents to the target are of the order of 0.03 to 0.05 microampere.

We have tentatively identified the following activities:

Cr: A rather weak activity of two periods is observed in this element after alpha-particle bombardment. A chemical separation of Cr, Mn, and Fe was made, and it was found that the short period activity, having a half-life of about 8.9 minutes, is due to an isotope of iron. It emits positrons. We suggest that the active isotope is Fe^{55}, formed by the reaction Cr^{52} (α, n) Fe^{55}. The long period radioelement is isotopic with Mn, and emits negative electrons, decaying with a period of about 160 minutes. This makes it seem likely that the activity is due to Mn^{56}, found by Fermi[3] to be produced in the bombardment of Mn with slow neutrons, and of Fe and Co with fast neutrons. The half-life of Mn^{56} is given by Fermi as 2.5 hours. The thick-target intensities of the activities, corrected to infinite bombarding time, are approximately in the ratio $Mn^{56} : Fe^{55} = 3 : 10$. Mn^{56} is produced in our work by the reaction Cr^{53} (α, p) Mn^{56}. The relative abundance of the Cr isotopes involved in these two reactions is Cr^{53}; $Cr^{52} = 10$ percent; 82 percent.[4]

Co: A great enhancement in the yield of Cu^{62} from the reaction Co^{59} (α, n) Cu^{62}, produced by the elimination of the alpha-particle energy loss in the cyclotron exit window, has enabled us to make a better measurement of the period than the one reported in our last communication.[2] Our present value of the half-life is 10.0 minutes, in agreement with that given by Pool, Cork, and Thornton[5] for the same isotope formed from Cu^{63} by the $(n, 2n)$ reaction.

Cu: We reported[2] the formation of Ga^{68} from Cu by the reaction Cu^{65} (α, n) Ga^{68}. The greater intensity now available shows the presence of a longer lived radioelement produced from Cu by alpha-particle bombardment, and has enabled us to make a more reliable measurement of the period of Ga^{68} than that already reported. A chemical separation of Cu, Zn, and Ga showed that both the radioelements produced in Cu are isotopic with Ga. Both emit positrons. The short period, measured in a sample of Cu bombarded for 15 minutes and measured immediately is 68 minutes, and is to be identified with Ga^{68}. The long period, measured in a Cu target bombarded for 3.5 hours and allowed to decay for 14 hours before being transferred to the electroscope, is 9.4 hours. We suggest that this latter activity is due to Ga^{66}, formed in the reaction Cu^{63} (α, n) Ga^{66}. The relative initial intensities are about $Ga^{68} : Ga^{66} = 10 : 4$, corrected to infinite bombarding time. We have studied the absorption in aluminum of the positrons from Ga^{68}, and find that the half-value thickness is about 0.12 g/cm², indicating a maximum energy of about 2.2 Mev.

As: In agreement with Snell,[6] we find a radioelement of half-life 6.3 minutes formed in As by alpha-particle bombardment. Snell has identified this activity as being due to Br^{78}.

We are very greatly indebted to Mr. R. C. Newton, who carried out for us the chemical separations mentioned above, and to Professor N. H. Furman for his helpful advice concerning them. Dr. M. G. White and Dr. M. C. Henderson have been chiefly responsible for the construction of the cyclotron with which these results were obtained.

W. J. HENDERSON
LOUIS N. RIDENOUR

Palmer Physical Laboratory,
Princeton University,
Princeton, N. J.,
June 16, 1937.

[1] W. J. Henderson, Ridenour, White and M. C. Henderson, Phys. Rev. **51**, 1107 (1937).
[2] Ridenour and W. J. Henderson, Phys. Rev. **51**, 1102 (1937).
[3] Amaldi *et al.* Proc. Roy. Soc. **A149**, 522 (1935).
[4] Hahn, Ber. d. D. Chem. Ges. **70**, 1 (1937).
[5] Pool, Cork, and Thornton, Phys. Rev. **51**, 890 (1937).
[6] Snell, Phys. Rev. **51**, 1011 A (1937).

Ionic Recombination in the Ionosphere

In a personal communication E. V. Appleton of the Cavendish Laboratory has called my attention to a point that was overlooked in my recent Letter to the Editor on the "Coefficient of Recombination of Gaseous Ions over an Extended Pressure Range."[1] In the letter I failed to consider the validity of the Thomson equation at extremely low pressures such as might apply to the ionosphere. There is nothing in the derivation of the Thomson equation which invalidates its applicability at lower pressures.[2] There is, however, a pressure below which the assumptions made in deducing the theory lead to values of the coefficient which are lower than the coefficient resulting from a process which is neglected in Thomson's theory. Thomson's theory assumes that ions will recombine if they come within the sphere of active attraction, $d = 2e^2/3kT$, of each other, and if when in that sphere one of the ions suffer a collision with a neutral molecule. At low pressures the chance of this molecular collision may be extremely remote for the coefficient ϵ giving this chance becomes very small. It is furthermore certain that if ions of opposite sign come within a distance r_0 of each other electron transfer will occur *without the added molecular impact*. Thus the Thomson mechanism for which $\alpha = \pi d^2 \epsilon (c_+^2 + c_-^2)^{\frac{1}{2}}$ must give way to another mechanism at pressures where $\pi d^2 \epsilon$ becomes comparable with πr_0^2.

While the mechanism of electron transfer characterizing ion recombination and defining r_0 has not been attacked by wave mechanics the process may be outlined as follows. The electron occupies a position of reduced potential energy in the molecule to which it is attached. On the approach of a positive ion there must exist at each distance of separation r between ions a finite chance of a transition of the electron over its small potential barrier into the vacant orbit of the positive ion. The overlapping electrostatic fields of the ions will materially facilitate this transfer, which in itself is rather high since the electron capture by the positive ion can proceed in a nonradiative manner the energy going to kinetic energy of separation of the resulting neutral molecules. Thus at each distance of

separation r there is on the average a time element τ characterizing a probable transition. Recombination depends on the chance that the ions are within r cm of each other for a time t sufficiently large compared to τ to insure transition. At a value of $r=r_0$ where τ is such that say 90 percent or more encounters result in transition we can then roughly fix the limiting collision radius.

In our present ignorance we can certainly set r_0 as greater than the kinetic theory diameter of the ion, and it may well be 10 times as large. One may then apply these considerations to the ionosphere. At 100 km Humphreys[3] gives the pressure as 0.0067 mm and the temperature of the order of 55 or more below °C. I will use −73°C. On this basis ϵ for $(O_2)_2^+$ will be 4.24×10^{-3} and $\alpha=1.61\times10^{-8}$. For the same gas $\alpha_r=\pi r_0^2(c_+^2+c_-^2)^{\frac{1}{2}}$ with $r_0=4\times10^{-8}$ and 4×10^{-7} cm, respectively, gives $\alpha_r=2\times10^{-10}$ and $\alpha_r=2\times10^{-8}$ *independent of the pressure*. Thus in the ionosphere unless $r_0>4\times10^{-7}$ cm the Thomson theory still applies.

Where electrical data from the ionosphere indicate values of α of the order of 10^{-10} one might assume that the recombination was no longer ionic but electronic.[4] This question can readily be answered if the oxygen content of the ionosphere is known. The work of Bradbury[5] gives the chance of electron attachment to O_2 molecules for a given electron energy. The ions once formed are stable. From the rate of ionization, the rate of electron attachment and the coefficient of recombination of ions the relative concentrations of the ions and electrons can be determined. If, as auroral spectra show, appreciable O_2 is present in the ionosphere it is probable that the negative carriers are largely ions.

LEONARD B. LOEB

University of California,
Berkeley, California,
June 7, 1937.

[1] L. B. Loeb, Phys. Rev. **51**, 1110 (1937).
[2] J. J. Thomson, *Conduction of Electricity Through Gases*. third edition. Vol. I pp. 40–47. L. B. Loeb, *Kinetic Theory of Gases*. second edition p. 592.
[3] W. J. Humphreys, *Physics of the Air*. second edition p. 70.
[4] C. Kenty, Phys. Rev. **32**, 624 (1928). F. Mahler, Bull. Am. Phys. Soc. **12**, abstract 55, p. 16 (1937).
[5] N. E. Bradbury, Phys. Rev. **44**, 885 (1933).

Evidence for the Simultaneous Ejection of Three Neutrons from Elements Bombarded with Fast Neutrons

It has recently been shown[1] that most elements when bombarded by very fast neutrons yield radioactive isotopes corresponding to the ejection from the stable nucleus of one neutron in addition to the bombarding particle. It now appears that in certain cases the impinging neutron can eject two neutrons in addition to itself. This phenomenon is best shown in the case of scandium.

The stable isotopes in this part of the periodic table are shown in Table I. Also included in this table are certain of the known radioactive isotopes. Scandium possesses normally a single stable isotope of mass number 45. When radiated by the fast neutrons (10 to 20 Mev) from lithium, which is bombarded by 6 Mev deuterons, scandium becomes strongly radioactive. Chemical separation of the bombarded specimen shows that there are two radioactive periods both positive in sign in the scandium precipitate. These half-life periods are approximately 4 hours and 52 hours and are in agreement with the results of Walke[2] who identified the same scandium isotopes by bombarding calcium with deuterons and potassium with alpha-particles.

TABLE I. *Stable and radioactive isotopes in the vicinity of scandium.*

	38	39	40	41	42	43	44	45	46
K	10 m	93%	.01%	7%	16 h				
Ca			97%		.7%	.1%	.2%	2.4 h	
Sc				53 m	4.1 h	4.0 h	52 h	100%	
Ti									>a 8.5%

The reactions are then as follows:

$$_{21}Sc^{45}+n\rightarrow{}_{21}Sc^{44}+n+n$$
$$_{21}Sc^{44}\rightarrow{}_{20}Ca^{44}+{}_{+1}e \qquad (52\text{ hr.}) \qquad (A)$$

$$_{21}Sc^{45}+n\rightarrow{}_{21}Sc^{43}+n+n+n$$
$$_{21}Sc^{43}\rightarrow{}_{20}Ca^{43}+{}_{+1}e \qquad (4\text{ hr.}) \qquad (B)$$

Although there is no previously known case where three neutrons are ejected from an excited nucleus, such a process is not inconsistent with the recent consideration of excited nuclei proposed by Bohr.

When scandium is bombarded by neutrons of energy under 8 Mev neither the 4 hour nor the 52 hour period is observed. In addition to these periods in scandium, fast neutron bombardment always yields by the emission of an alpha-particle the 16 hour activity in potassium attributed to isotope K^{42}.

Among other elements that might show this phenomenon of multiple neutron ejection are copper and fluorine. In both cases there is evidence that the process occurs but the identification cannot be made as certain as in the case of scandium. The periods in fluorine corresponding to the ejection of two and three neutrons (i.e., F^{18} and F^{17}) are 108 min. and 1.2 min., respectively. The similar isotopes in copper are Cu^{62} and Cu^{61} with half-life periods of 10 min. and 3.5 hr. The 3.5 hour period of Cu^{61} is very weak compared to the strong 12.5 hour period of Cu^{64}.

This work has been made possible by a grant from the Horace H. Rackham Trust Fund.

M. L. POOL*
J. M. CORK
R. L. THORNTON

Department of Physics,
University of Michigan,
Ann Arbor, Michigan,
June 14, 1937.

[1] Pool, Cork and Thornton, Phys. Rev. **51**, 890 (1937).
[2] Walke, Phys. Rev. **51**, 439 (1937).
* Elizabeth Clay Howald Scholar.

On the Existence of Heavy Electrons

Different observers[1] believe they have found evidence for the existence of charged particles whose mass amounts probably to about fifty times the electron mass. Furthermore these particles seem to behave according to the Bethe-Heitler theory.[2]

The writer wishes to call attention to an explanation of the nuclear forces, given as early as 1934, by Yukawa,[3] which predicts particles of this sort.

Independently of Yukawa the writer arrived at the same conclusion: Kemmer has shown recently[4] that the formal conception of field theory proposed by the author[5]

leads to great difficulties, if the proposed interaction energies have singular character. Interaction energies of nonsingular character can most easily be introduced by assuming the existence of some tensor field differing from that of ordinary radiation.

We describe *matter* by a 16 component spinor ψ, whose first four components refer to the *electron state*, the second four functions to the *neutrino state*, the third group to the *proton state* and the last four components to the *neutron state of matter*. Each of these states is defined by the values of a set of four indices (*charge numbers*) $(\alpha, \beta, \gamma, \delta)$ which have respectively the values $(1, 0, 0, 1)$, $(0, 1, 0, 1)$, $(1, 0, 1, 0)$ and $(0, 1, 1, 0)$. Quantum theory associates *particles* with this field which we denote by the same symbol ψ. They have the spin 1/2 and obey Fermi *statistics*. Their *antiparticles* are to be described as holes according to Dirac's idea and designated by $-\psi$. They have the same charge numbers as the particles but with reversed sign. If e represents the elementary charge $e\alpha$ is the *electric charge* of the particle in the state given by $\psi(\alpha, \beta, \gamma, \delta)$. $\gamma = 1$ or 0 indicates whether the particle has *heavy mass* ($\sim$2000) or light mass ($\sim$0 to 1). Matter satisfies evidently the relation $\alpha+\beta=\gamma+\delta=1$. The indices β and δ can be called *neutrino charge* and *light mass number*.

The known form of radiation is described by a tensor field A of four components (the vector potential). We attribute to its particles (photons), designated analogously by $A(\alpha, \beta, \gamma, \delta)$ the charge numbers 0. Emission of a photon by matter is due to an interaction term proportional to $e\alpha$ and can be described by the reaction:

$$\psi(\alpha, \beta, \gamma, \delta) \rightarrow \psi(\alpha, \beta, \gamma, \delta) + A(0, 0, 0, 0). \qquad (1)$$

The components of the A field satisfy Poisson's equation, the charge density being expressed by a suitably chosen generalized Dirac matrix $P = e\psi^{+}\Lambda\psi$ (cf. reference 5). We generalize Poisson's equation, introducing the fundamental length λ in the form:

$$\left(\Delta - \frac{1}{c^2}\frac{\partial^2}{\partial t^2} - \Sigma\frac{1}{\lambda^2}\right)A = -P. \qquad (2)$$

A is now a tensor of more than four components. Σ is a matrix operating on the tensor indices analogously to the way Dirac's matrices act on the spin indices of ψ. We assume for simplicity A to have five components. Furthermore let Σ be of such a form that the four first components which represent a four vector satisfy the ordinary Poisson equation ($\Sigma = 0$), while the fifth component (a scalar) satisfies Eq. (2) with $\Sigma = 1$. In a nonrelativistic approximation the four-vector part gives the Coulomb potential, while the scalar part gives a static interaction term between particles of the form $(fe^2/r)\exp(-r/\lambda)$. f is a numerical factor, depending on the choice of the Λ matrix. A suitable choice (see reference 5) of the generalized Dirac matrices Λ gives the electrostatic interaction between charged matter particles plus the Heisenberg, Majorana, Wigner and Bartlett interactions between heavy matter particles[6] and the different interactions between heavy and light matter particles (β-decay, etc.) discussed by the author. The Heisenberg interaction seems to demand a second order tensor field A.

The *particles* associated with this *generalized radiation* field have integer spins and obey Bose statistics. Those components for which $\Sigma \neq 0$ have a rest mass $m = h/c\lambda \neq 0$.

We generalize the *conservation law* of charge numbers expressed in Eq. (1): Then the A particle which appears in nuclear reactions has the charge numbers $(1, -1, 0, 0)$. Radiation satisfies evidently the relations $\alpha+\beta=\gamma+\delta=0$. *Antiparticles* have of course once more the charge numbers with reversed sign. There are naturally no antiphotons as the charge numbers of the four-vector field are identically 0. β^{+} decay can be written down as the result of two successive reactions:

$$\psi(1, 0, 1, 0) \rightarrow \psi'(0, 1, 1, 0) + A(1, -1, 0, 0), \qquad (3)$$

$$A(1, -1, 0, 0) \rightarrow \psi''(1, 0, 0, 1) + (-\psi'''(0, 1, 0, 1)). \qquad (4)$$

A proton ψ decomposes into a neutron ψ' and a positively charged *Bose electron* A, which in turn decomposes into an ordinary (positive) electron ψ'' and an antineutrino—ψ'''. As, even in the β-spectra of highest known energy (24 mc^2), those Bose electrons have never been observed, their mass must be greater than 24 electron masses. Yukawa from other considerations estimates about fifty electron masses.

If the corresponding field component has scalar character, the Pauli-Weisskopf theory[7] can be applied. The interaction between this field and the four-vector field (electromagnetic field) leads to a formula differing but little from the Bethe-Heitler theory.[2]

It seems highly probable that Street and Stevenson, and Neddermeyer and Anderson [1] have actually discovered a *new elementary particle*, which has been prediced by theory.

This particle is unstable and can only be of secondary origin, its mass being greater than the sum of the masses of electron plus neutrino. There exist very probably also other particles for example: $A(0, 0, 1, -1)$.

It is interesting to note that we have a nonlinear field theory, the field having tensorial and spinorial components. The one set is generalized Maxwell equations (2), which are quadratic in the A's if the electromagnetic interaction is included in (2) and quadratic in the ψ's. The other set has the form of generalized Dirac equations, proposed by the author, and contains linear terms in ψ and bilinear ones in the ψ's and A's.

The writer is indebted to his colleagues Professor J. Weigle (Genève) and G. Wentzel (Zuerich)[8] for many a helpful discussion.

E. C. G. STUECKELBERG

Institut de Physique,
Genève, Switzerland,
June 6, 1937.

[1] J. C. Street and E. C. Stevenson, Bull. Am. Phys. Soc. **12**, 13 (1937); S. H. Neddermeyer and C. D. Anderson, Phys. Rev. **51**, 886 (1937).
[2] H. Bethe and W. Heitler, Proc. Roy. Soc. **A146**, 83 (1934).
[3] H. Yukawa, Proc. Phys. Math. Soc. Japan **17**, 48 (1937).
[4] N. Kemmer, Helv. Phys. Acta **10**, 47 (1937).
[5] E. C. G. Stueckelberg, Nature **137**, 1032 (1936); CR. de la Soc. phys. et sc. nat. Genève **53**, 64 (1936); Helv. Phys. Acta **9**, 389 and 533 (1936). The matrices Λ in this note are the Λ and the Ω matrices in the former theory. Instead of the conservation law of charge numbers the author introduced in these former publications a certain relationship between particles and their antiparticles.
[6] See, for example, the different publications of the Leipzig Institute: S. Fluegge, Zeits. f. Physik **105**, 522 (1937); H. Volz, Zeits. f. Physik **105**, 537 (1937); H. Euler, Zeits. f. Physik **105**, 553 (1937).
[7] W. Pauli and V. Weisskopf, Helv. Phys. Acta **7**, 709 (1934); W. Pauli, Ann. Inst. H. Poincaré p. 137 (1936).
[8] G. Wentzel, Zeits. f. Physik **104**, 34 (1936) has also introduced new particles, but he attributed to them a mass near that of the proton (Bose protons and Bose neutrons).